## Title

# Surgically Assisted Rapid Palatal Expansion vs. Segmental Le Fort I Osteotomy: An Analysis of Transverse Stability Using Cone Beam Computed Tomography



**Author**
Yao, William M.

**Publication Date**
2011

Peer reviewed|Thesis/dissertation

Surgically Assisted Rapid Palatal Expansion vs. Segmental Le Fort I Osteotomy: An Analysis of Transverse Stability Using Cone Beam Computed Tomography

by

William M. Yao, DDS

THESIS

Submitted in partial satisfaction of the requirements for the degree of

MASTER OF SCIENCE

in

Oral and Craniofacial Sciences

in the

GRADUATE DIVISION

of the

UNIVERSITY OF CALIFORNIA, SAN FRANCISCO

[redacted]

## DEDICATION

To my wife Dana and our son Elias, whose unconditional love and encouragement have carried me through every day of this journey.

## ACKNOWLEDGMENTS

I would like to express my gratitude to the people who made this work possible.

Thank you to each of my committee members for their generous time and support. Dr. Janice Lee who graciously offered her surgical expertise at every juncture; Dr. John Huang whose incomparable knowledge of 3D imaging was instrumental in the development of my ideas; Dr. Art Miller's kindness and daily encouragement inspired me to do my best work. I consider myself blessed to have worked with all these wonderful mentors.

I would also like to thank Daniel Hardy, Thanh Phan and Sona Bekmezian for their countless hours in front of a computer on my behalf, and my fellow co-residents who have had to listen to my spiel over and over again. I am truly grateful to have had the opportunity to work with each of these amazing people.

## ABSTRACT

### Surgically Assisted Rapid Palatal Expansion vs. Segmental Le Fort I Osteotomy: An Analysis of Transverse Stability Using Cone Beam Computed Tomography

**William M. Yao, DDS**

**OBJECTIVE**: To examine the immediate and subsequent skeletal and dental effects of surgical widening of the maxilla via two orthognathic procedures, Segmental Le Fort Osteotomy and Surgically Assisted Rapid Palatal Expansion (SARPE), using cone beam computed tomography (CBCT).

**METHODS**: A total of thirteen subjects satisfied the inclusion criteria for this study (9 Le Fort and 4 SARPE). Patient ages averaged 28.4 years (range 17.1 – 45.3) in the Le Fort group and 19.2 years (range 17.0 – 23.2) in the SARPE group. Three CBCT scans were taken at time-points defined as follows: Le Fort (T0 = preoperative, T1 = post-operative, T2 = 6+ months postoperative) and SARPE (T0 = preoperative, T1 = post-expansion retention, T2 = 6+ months). Skeletal and dental width measurements were recorded using 3D imaging software, Anatomage InVivo 5.x (Anatomage, San Jose, CA).

**CONCLUSIONS**: Surgical expansion of the maxilla in the transverse dimension without performing separation of the pterygomaxillary junction resulted in less than 1 mm of skeletal expansion. During expansion with a multisegmental Le Fort procedure, more expansion occurred skeletally than dentally, with a posterior and anterior ratio of dental:skeletal expansion of 0.70 and 0.58, respectively. During expansion with a SARPE procedure, significantly more expansion occurred dentally than skeletally, with a posterior and anterior ratio of dental:skeletal expansion of 25.19 and 31.80, respectively. In both groups, relapse was more dental than skeletal, with the SARPE group showing a higher ratio of dental:skeletal change. The forces generated by expansion via a Hyrax appliance in a SARPE procedure may cause slight increase in width from T1 to T2 due to changes in the biomechanical system resulting from osteotomy.

**TABLE OF CONTENTS**

LIST OF FIGURES

LIST OF TABLES

# INTRODUCTION

## Purpose

To understand the immediate and subsequent skeletal effects of surgical widening of the maxilla via two orthognathic procedures, Segmental Le Fort Osteotomy and Surgically assisted Rapid Palatal Expansion (SARPE), using cone beam computed tomography (CBCT).

## Specific Aims

- **Part One:** Establish a protocol for using CBCT to measure transverse changes in the maxilla
  - Define landmarks within the maxillary complex to measure transverse changes in the maxilla
  - Evaluate reliability of identifying landmarks

- **Part Two:** Describe relative maxillary skeletal and dental transverse changes as a result of two orthognathic procedures, Segmental Le Fort Osteotomy and Surgically Assisted Rapid Palatal Expansion (SARPE).

## Hypotheses

- The greater and lesser palatine canals (GP and LP), and the piriform rim are structures that can be used to reliably measure transverse changes in the maxilla
- The ratio of transverse skeletal expansion/relapse to dentoalveolar expansion/relapse is dependent on the amount and type of surgical expansion

## Premise

A recent U.S. Public Health Survey concluded that the prevalence of maxillary constriction is 9.4% of the general population with little change from 8-50 years of age.[1] Proffit[2] has reported that as high as 30% of adults that seek orthodontic treatment for dentofacial deformity have a component of maxillary transverse deficiency (MTD). Clinical manifestations of MTD can include posterior crossbite, a narrow, tapered palatal vault and/or large negative spaces near the corner of the mouth termed buccal corridors.[3] In a growing patient, orthopedic intervention is especially effective in the correction of MTD because the midline palatal suture has not completely fused, allowing for significant separation of the palatine processes and expansion of the maxilla in the transverse dimension. [3-6] In a non-growing patient, or in a patient whose midline palatal suture has fused, orthognathic surgery is indicated for expansion of the maxilla.[7]

According to the Hierarchy of Stability of surgical-orthodontic procedures, described by Proffit and Bailey,[8] surgical expansion of the maxilla in the transverse dimension is the least stable of all the orthognathic corrections. Surgical correction of MTD is generally accomplished with a SARPE or a 2-piece Le Fort I osteotomy; variations exist with respect to surgical procedure and type of appliance used.[9,10] Depending on the amount of correction desired, or whether the deficiency involves other planes of space, the orthodontic-surgical team will choose the appropriate procedure.

Previous studies have demonstrated post-surgical relapse in patients ranging from 5-28% in the intercanine region and approximately 50% in the intermolar region, in patients who undergo 2-piece Le Fort osteotomy. [8,10,11] For patients with correction via a SARPE procedure, studies have shown relapse ranging from 0-23% in the intercanine distance and 7-33% in the intermolar distance. [11-18] The wide range of reported results may be related to variations in surgical procedure, and the methods by which the transverse changes are measured. Previous studies relied primarily on dental measurements and posterior-anterior (PA) cephalometric projections, which may not clearly represent the changes that are occurring in the maxillary bone.

Although clinicians concur with the clinical applications of surgical expansion of the maxilla, numerous disagreements exist regarding the outcomes of the procedure and its stability over time. The introduction of three-dimensional imaging has provided a means to gain additional information regarding the outcome of such surgical corrections. This study examined the effects of surgical transverse expansion on the dental and skeletal components of the maxilla, incorporating landmarks that are meant to implicitly represent changes in the palate.

**Etiology of Maxillary Constriction**

Maxillary constriction is defined as a maxillary width that is narrower than the norm for a particular age group.[19,20] A deficiency in the width of the maxilla may have a genetic cause, an environmental cause, or a combination of the two factors. [21] In Marfan's syndrome, patients characteristically have a high-arched palate in association with a constricted maxilla.[22] In patients with craniofacial syndromes such as the Velocardiofacial syndrome, a constricted maxilla may be inherited. [23] Patients who have a cleft palate, either isolated or associated with a syndrome, often have a hypoplastic and constricted maxilla. [24] Other syndromes which often have maxillary constriction as a feature include the Klippel-Feil syndrome, congenital piriform aperture stenosis, craniosynostosis (Apert's, Crouzon's syndrome, Carpenter's), Treacher Collins, and Duchenne muscular dystrophy.[25]

In other cases, maxillary constriction is thought to be a result of environmental influences, as seen with patients who have an abnormal function of the orofacial complex or respiratory system. Several authors have suggested that abnormal breathing patterns alter maxillary development and may result in abnormal maxillary growth.[26] In a study by Harvold, Cheirici and Vargervik[27], they blocked the nasal airway in Rhesus monkeys, converting them into obligate mouth breathers of varying degrees, and observed changes to the tongue posture, mandibular position and maxillary development; they found a decrease in the transverse development of the maxilla.

The overall consensus is that the etiology of maxillary constriction is multifactorial. Some authors state that the maxillary skeletal base, dentoalveolar processes, and function play a role in the development of the transverse discrepancy. [1,28-30]

**Orthognathic Surgery to Correct Maxillary Transverse Deficiency**

In the absence of a patent midpalatal suture and the availability of growth potential, the maxilla must be surgically manipulated to correct maxillary deficiency. Proffit[21] reports that “by the late teens, interdigitation and areas of bony bridging across the suture develop to the point that maxillary expansion becomes impossible.” This idea is supported by the histological studies of Melsen[6] showing the palatal suture at different stages of development, and it’s closure in the teenage years.

**Indications:**

There are two orthognathic procedures that are used widely for the widening of the maxilla; they are the Segmental Le Fort Osteotomy and the SARPE. There is lack of consensus among orthodontists and surgeons regarding clinical indications for a Segmental Le Fort Osteotomy versus a SARPE procedure for correction of transverse discrepancy.

A segmental Le Fort Osteotomy is often the surgery of choice when the patient is in need of correction in multiple planes of space.[31] When a segmental Le Fort is planned, it is preferred that the amount of transverse discrepancy is no more than 6-7 mm; this value is based on previous studies which demonstrate that for corrections larger than 6-7 mm, a SARPE procedure is more stable.[32-34] Proffit[35] believes that the decreased stability in expansions of greater than 7mm with a segmental osteotomy is related to stretching of the palatal tissues, immediate expansion, and less rigid retention.

The following indications for a SARPE procedure have been cited in the literature:[25] 1) To increase the maxillary arch perimeter and correct posterior cross-bite when no additional jaw movements are planned; 2) to provide space for a crowded dentition when extractions are not indicated; 3) to widen the maxillary hypoplasia associated with palatal clefts 4) to reduce buccal corridors when smiling; and 5) to overcome sutural resistance when orthopedic maxillary expansion has failed.

**Amount of expansion:**

Betts[9] and Vanarsdall[20] suggest that maxillomandibular discrepancies of 5 mm or less can be treated using orthodontic methods alone with reasonably stable results. When the maxillomandibular discrepancy is greater than 5 mm, surgical assistance is recommended.[36] Several authors believe that expansion of more than 6-7 mm with a segmental Le Fort osteotomy is unstable,[32-34,37] and recommend that a SARPE procedure be considered if large corrections of greater than 7 mm are planned. There are no studies elucidating the reasons for these differences. It has been postulated that areas of soft-tissue resistance, bony resistance, amount of expansion, rate of expansion, type and duration of retention, and surgical procedure all play a role in determining skeletal and dentoalveolar stability of the final outcome.[8,10,25,34,35,38]

**Surgical Technique:**

Considerable variation exists with respect to surgical technique. The three principal areas of vertical and horizontal maxillary support are the nasomaxillary, zygomaticomaxillary, and pterygomaxillary buttresses.[39] The diverse maxillary osteotomies that have been empirically proposed to facilitate lateral palatal expansion reflect the conflicting opinions about the areas of resistance in the craniofacial skeleton.[40] Early reports suggested the midpalatal suture as the primary area of resistance to lateral expansion forces.[6,41,42] Later reports implicated the zygomatic buttress and the pterygomaxillary junction as additional sites of resistance.[7,43,44]

The first reported surgical technique involving a mid-palatal split osteotomy was described by Brown.[45] For the remaining 1st half of the 20th century, there was no significant evolution of the technique. In 1959, Kole[46] used selective sectioning of the cortical bone to reduce resistance to orthodontic forces. Traditional techniques favoring a midpalatal osteotomy as a principal surgical adjunct derive from histological studies by Timms[47] in 1968, implicating the fused midpalatal suture as the primary area of resistance to expansion forces. In contrast, studies by Isaacson *et al*.,[48] downplayed the role of the midpalatal suture as a source of resistance. These studies set off a multiplicity of osteotomies aimed at promoting a physical separation of the maxillary halves while minimizing resistance and, therefore, dentoalveolar effects.[40]

In 1969, Converse and Horowitz[49] advocated the use of corticotomies on both the labial and palatal surfaces to further reduce resistance to expansion forces. In 1972, Steinhauser[50] described the use of a LeFort I type osetotomy with use of an iliac bone graft for correction of maxillary constriction. In 1976, Kennedy[51] used selected maxillary osteotomies in Rhesus monkeys to study the effects on maxillary expansion. He performed lateral maxillary osteotomies and pterygomaxillary osteotomies with and without palatal osteotomy versus unoperated controls and versus palatal osteotomy only. He concluded that there was a significant difference in lateral movement, and that eliminating resistance using all the described osteotomies allowed the basal bone of the maxilla to move laterally.[51]

Timms and Vero[42] advocated a staged approach in determining the ideal number of osteotomies to include. Stage 1 includes a median palatal osteotomy and is recommended for patients of 25 years and older. Stage 2 includes a median palatal osteotomy and a bilateral maxillary osteotomy, and is recommended for patients of 30 years and older. Stage 3 includes a median palatal osteotomy, bilateral maxillary osteotomy and anterior osteotomy, and is reserved for patients of 40 years and older. In Fonseca's publication, Betts[39] advocated sectioning all articulations and areas of resistance, including lateral osteotomies, median osteotomies, anterior osteotomies, and releases from the nasal septum and pterygoid plates.

Lehman *et al.,*[52] advocated a more conservative and simplified approach. According to their findings, removing resistance at the zygomatic buttress is sufficient to significantly reduce resistance. Glassman *et al.,* also supported a similar conservative approach.[53] Both Bays and Greco[17] and Northway and Meade[15] warned against separation at the pterygoid junction in order to prevent fracture of the plates. Pogrel *et al.,*[18] recommended only a midplatal osteotomy paired with lateral osteotomies to reduce resistance. In addition to the locations of the osteotomies, there are also differences in the design of the palatal osteotomy, varying from a single midline split, to paramedian cuts or to horseshoe-shaped osteotomies.[38]

It is apparent in reviewing the available literature that there is no consensus regarding the type or extent of surgical technique to widen the maxilla. There is also no conclusive evidence regarding the areas of highest resistance to maxillary expansion. The location and number of osteotomies used for surgical maxillary expansion reflect the controversy regarding the primary areas of resistance to expansion in the craniofacial skeleton.[39] To date, surgical technique is highly variable with respect to individual diagnosis and treatment goals.

**Biomechanics of Maxillary Expansion**

There have been several studies about the force levels and force distribution associated with widening of the maxilla. Chaconas *et al.,*[54] studied the force distribution to the maxilla during active expansion. This study revealed that the force levels distributed to the maxilla varies greatly and that a single activation of a fixed expansion appliance, such as a Hyrax or a Haas appliance, can produce 3-10 lbs. of force, with a rapid decay followed by a slower decay curve.[54] Bishara[30] examined the bone quality of the midpalatal suture during maxillary expansion and showed that there is a change in the mineral content within the suture. As expansion forces accumulate, the mineral content decreases; following active expansion, the mineral content within the suture rapidly increases returning to baseline levels within 3 months.[30]

Shetty *et al.,* [40] used photoelastic bone analogs to characterize the principal midfacial stress trajectories associated with expansion forces to the maxilla. Based on the findings of the study, it is reasonable to conclude that the effectiveness of maxillary expansion is significantly influenced by the patency of the midpalatal and pterygomaxillary articulations.[40] In 2003, Jafari *et al*.,[55] used finite element modeling to study the stress distributions in the craniofacial complex as a result of maxillary expansion. They found that transverse expansive forces not only produced stress at the intermaxillary sutures, but also high forces on other structures of the craniofacial complex, particularly the sphenoid and zygomatic bones.[55] More recently, Holberg *et al.,*[56] used finite element modeling to investigate the stresses in the midface and the cranial base during SARPE. The study concluded that separation at the pterygomaxillary junction appears to be a reasonable and necessary measure to decrease unwanted stresses during palatal expansion.[56]

There are few studies related to the skeletal dynamics and biomechanics related to the widening of the maxilla. Wertz[5] showed that there was greater expansion in the anterior maxilla than in the posterior maxilla; vertically, more expansion was observed at the level of the dentition when compared to the components of the maxillary skeleton and nasal floor. Bailey *et al.,*[33] showed that more expansion can be obtained in the posterior maxilla when a segmental Le Fort I osteotomy is used for transverse correction. Braun *et al.,*[57] used laser holography to visualize the microdisplacements in the bones of the craniofacial complex during expansion of the maxilla in an attempt to define the centers of rotation of the maxillary halves. They approximated the locus of the center of rotation during initial displacement of the dentomaxillary complex to be at the area of the frontonasal suture. Using the data from a previous study by Lee *et al.,*[58] describing the centers of resistance in the dentomaxillary complex in the sagittal and frontal views, Braun *et al.,*[57] related their findings to the findings of the Lee *et al.,* study and diagrammed the force systems as related to maxillary expansion. It is important to note that the study by Braun *et al.,*[57] did not involve surgical intervention to reduce resistance to expansion forces, which would alter the loci of the centers of resistance and rotation, thereby redefining the entire force system.

In reviewing the current literature, it is clear that there are changes occurring in the craniofacial complex as a result of imposing expansive forces on the maxilla. However, the dynamics and particular biomechanics of the system is not well understood.

**Measurement of Maxillary Transverse Expansion**

Until recently, transverse changes in the maxilla have been assessed by clinical evaluation, plaster model analysis, or two-dimensional cephalograms.[38] Clinical evaluation includes assessment of the maxillary arch form and symmetry, shape of the palatal vault, width of buccal corridors on smiling, occlusion, and subjective reports on changes to nasal respiration. Study models have been used extensively in the literature to evaluate changes in the maxilla. Several indexes have been proposed by various authors to measure lateral deficiencies or changes; the most common include indexes by Pont, Linder-Harth, and Korkhaus. [25] Although these indexes offer a guide to diagnosing and evaluating maxillary problems related to the transverse dimension, they are population specific and not completely reliable.[25] Redmond[59] has shown that digital models are an accurate and reliable substitute for study models to measure changes in the maxillary arch. Digital models offer an additional tool that can be used to evaluate changes to the axial inclination of the teeth, produce occlusograms to analyze changes in the coordination of the arch forms, and the cross-sectional views allows clinicians to better distinguish between changes in the teeth and the apical base skeleton.[59]

Lehman *et al.,* have advocated the use of the palatal radiograph as a tool to monitor the bony changes in the midpalatal suture.[52] This method, however, is unreliable because of superimposition of other bony structures on the midpalatal suture, and the inability to adequately visualize the posterior aspect of the suture.[25] Haas created one of the first analyses based on 45 patients with maxillary deficiency.[60] In his study, Haas used serial PA cephalograms superimposed on each other, and constructed tangents from which he derived linear measurements to represent maxillary changes in the lateral dimension. Betts *et al.,*[36] also advocated the use of PA cephalograms to evaluate changes to the lateral dimension of the maxilla. Using cephalometric landmarks as described by Ricketts,[19] they presented 2 methods for quantifying MTD: the maxillomandibular width differential and the maxillomandibular transverse differential index (Figure 1).

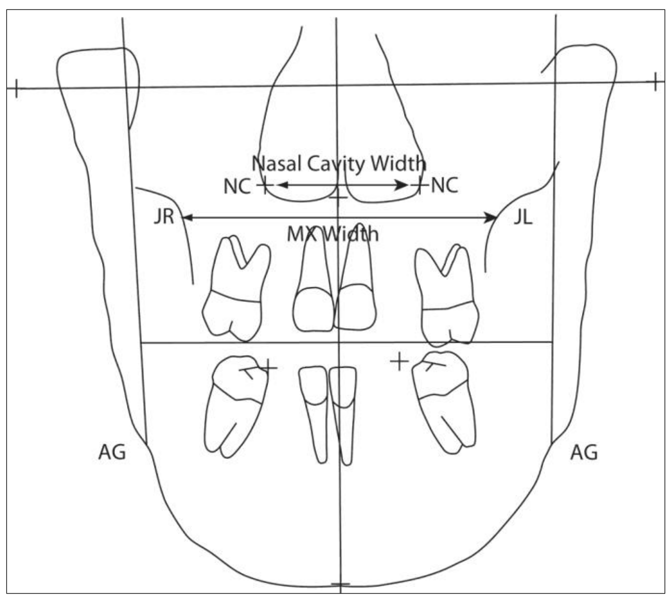


**Figure 1: The maxillomandibular width differential (Abbreviations: AG is antegonial notch; JR/JL iis jugule point, NC is nasal cavity.[19])**

Baccetti and Mcnamara[61] have also devised a system for measuring maxillary expansion based on PA cephalograms (Figure 2) in which they identify pairs of bilateral bony landmarks, connecting them to arrive at linear measurements at several vertical levels of the cephalogram.


**Figure 2: Using PA cephalogram to measure maxillary base width.** [61]

Several disadvantages of analyzing transverse changes in the maxilla using PA cephalograms include head posture of the patient in the cephalostat, magnification error, accuracy of superimposition techniques, and inadequate visualization of landmarks. In surgical correction of MTD, the location of the osteotomy has a potential of obscuring the view of vital structures that are used in several of the aforementioned analyses, most notably the midpalatal suture and in the area of jugale, near which the lateral osteotomy often occurs.

The introduction of three-dimensional imaging has provided a tool to overcome several of the disadvantages mentioned above. The use of computed tomography (CT) has been shown to be a reliable means to evaluate changes in maxillary dimensions following SARPE.[62] Loddi *et al.,*[63] used computed tomography to evaluate changes in the midpalatal suture following a SARPE procedure. Goldenberg *et al.,*[64] studied transverse changes in the maxilla using computed tomography to measure from anatomic landmarks such as the maxillary sinus and the greater palatine canal. Several disadvantages of traditional CT imaging should be mentioned, including high radiation dose, window setting scan noise, artifacts, spatial uniformity, resolution, relative difficulty of access, and high cost.[65] The process of obtaining a full scan is lengthy, primarily because each trans-axial slice is captured separately. Movement of the patient during the imaging process can result in a distorted reconstruction of the image which is difficult to analyze. Finally, the radiation exposure to the patient is very high due to the extended time needed to complete a scan.[66]

Cone beam computed tomography (CBCT) was introduced in 2001 as an alternative to traditional CT. CBCT has offered many solutions to the limitations of traditional CT in dentomaxillofacial applications. The reduced physical size and cost of the unit are major advantages. The cone shaped beam allows for shorter imaging times and lower radiation exposure.[67] Scan times average 10 seconds using the Hitachi CB MercuRay™ CBCT scanner (Hitachi

Medical Corporation, Tokyo, Japan) which decreases the likelihood of distortion due to patient movement. The radiation exposure is similar to the range of a standard dental radiograph series.[66-69] Spatial resolution of CBCT is equivalent to the resolution of a standard spiral CT, but at a significantly reduced radiation dosage. The effective dose of a CBCT is 200-400 μSv versus a spiral CT at 2000 μSv.[70] A thorough review of CBCT versus CT concluded that while CT has technical advantages in critical fields such as pulmonology and cardiology, CBCT is an adequate, lower dose method of obtaining reliable three-dimensional images on the craniofacial region.[71]

The accuracy of measurements obtained from CT images has been investigated by several authors. Cavalcanti *et al*., concluded that the measurements taken from CT images were very accurate when compared to physical measurements of dry skulls.[72] They reported measurement error ranging from 0.45-1.44%. Stratemann reported highly accurate measurements in all dimensions with measurement error ranging from 0.09-0.30%.[73] Kragskov *et al,.*[74] found that the overall variation was higher when the same points were studied on cephalograms as compared to CT. Landmark points related to a frontal cephalogram showed even higher variation, ranging from approximately 1-3mm. These studies have confirmed that the measurements obtained from reconstructed CBCT images are anatomically accurate and offer many advantages to traditional two-dimensional views.

## Reason for Further Investigation

In 2007 and 2008, Goldenberg *et al.,*[64,75] reported on the use of computed tomography to evaluate transverse changes in the maxilla after SARPE. Their study compared the amount of Hyrax appliance opening to the amount of skeletal maxillary expansion as defined by several landmarks within the maxillary complex. Their study did not, however, evaluate relapse or compare skeletal changes within the maxilla to dental changes occurring in the same patients.

The present study builds on the ideas of Goldenberg *et al.,* [64,75] by using CBCT to evaluate skeletal and dental expansion and relapse in the maxilla as a result of Segmental Le Fort Osteotmy and SARPE procedures.

## MATERIALS AND METHODS

This study was executed in two parts. The first part of the study was dedicated to designing a protocol for measuring transverse changes in the maxilla using 3-D CBCT visualization software (Anatomage InVivo Dental 5.0, Inc, San Jose, CA), and to test the reliability of the protocol and its associated measurements. The second part of the study used acceptable measurements defined in the first part of the study to evaluate the transverse skeletal and dental changes in a sample of patients that underwent surgical widening of the maxilla.

## Part One: Measurement Protocol and Reliability of Methods

A pilot group of four patients was used to develop a measurement protocol for measuring transverse changes using CBCT data and Anatomage 5.x software.  The data were analyzed to determine the most statistically reliable measurements. The pilot study was structured as follows:

### Pliot Study

- Three blinded and calibrated observers (author plus two research assistants)
- Two masked Le Fort subjects evaluated at 3 time-points (T0, T1, T2)
- Two masked SARPE subjects evaluated at 3 time-points (T0,T1,T2)
- Three measurement recording sessions, each two weeks apart
- 18 measurements per subject

### Data analysis

To date, several methods exist for studying the stability of surgical maxillary expansion in the transverse dimension.[3,34,52,60,61,64,75] The most prevalent methods involve measuring the intermolar and intercanine distances on plaster models.  Other methods include using PA cephalograms and measuring the distance between the jugale points, bilaterally.  However, little work has been done using three-dimensional imaging to quantify the skeletal effects of surgical correction of MTD.

We chose to create an analysis based on using internal structures of the maxilla to study the effects of surgical maxillary expansion and its stability. Our analysis used CBCT images in DICOM format loaded into Anatomage InVivo 5.x software. The data were analyzed using a volumetric view as well as a multiplanar view (Figure 3).

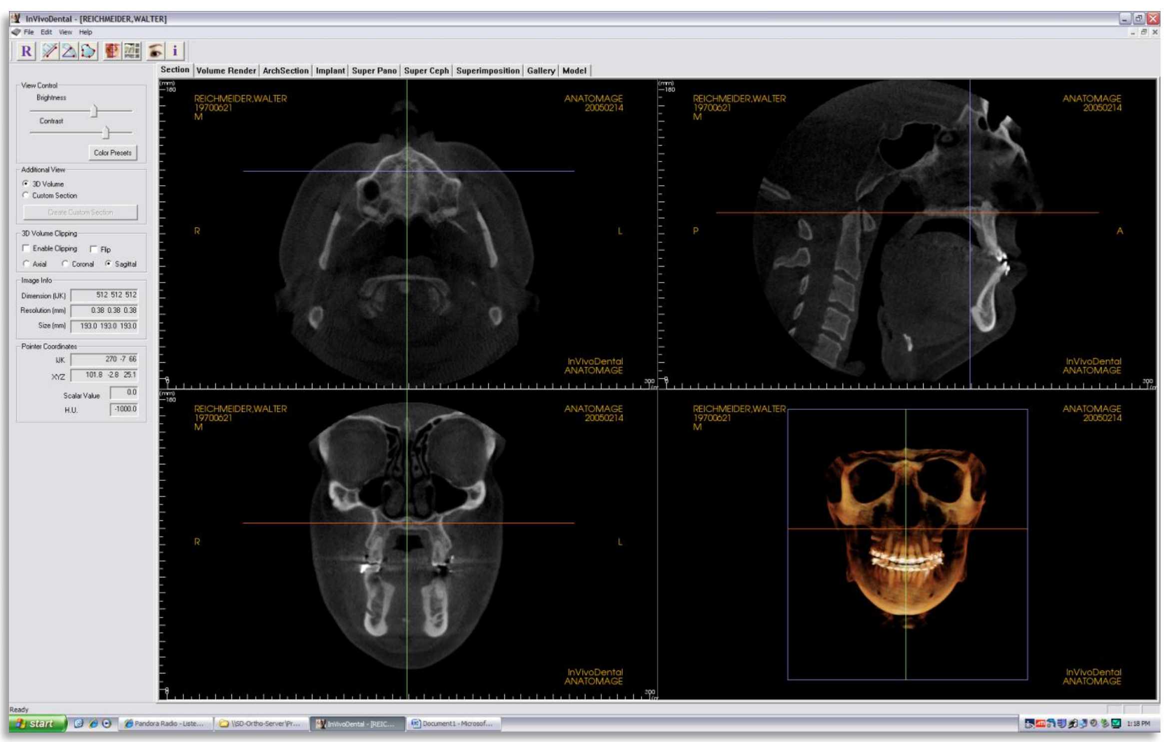


**Figure 3: Screen display demonstrating the horizontal, coronal, and sagittal planes as well as a surface rendered volumetric view of one patient as displayed using the Anatomage software.**

**Scan Orientation**

Each of the scans was assigned a number using a random number generator (Random.org, Dublin, Irelend). The scans were then loaded into the software and analyzed with the patient, time-point, and type of surgery masked. Prior to analysis, each scan was oriented using three reference planes aligned to pass through specific anatomic landmarks. A similar method was described in previous theses by Schlicher *et al.,* 2007 and Laurent *et al.,* 2008, using Dolphin Imaging Software (Dolphin, Chatsworth, California). All scans were oriented according to the following protocol:

**Scan Orientation Protocol**

**X-axis** = a plane passing through left and right zygomatico-frontal sutures

**Y-axis** = a plane passing through the crista galli superiorly and bisecting the clivus inferiorly

**Z-axis** = a plane passing through Sella and Nasion

1. Open InVivo 5.x software by Anatomage Inc.
2. Load DICOM data for research subject
3. Select the "Section" tab to load the multiplanar view
4. Select the "Layout" option
5. Click "Equal sizes"
6. On the sidebar, select 3D volume as the "additional view"
7. Select the "Orientation" button on the main toolbar

8. Use the orientation widget tool to orient the data (Figure 4)

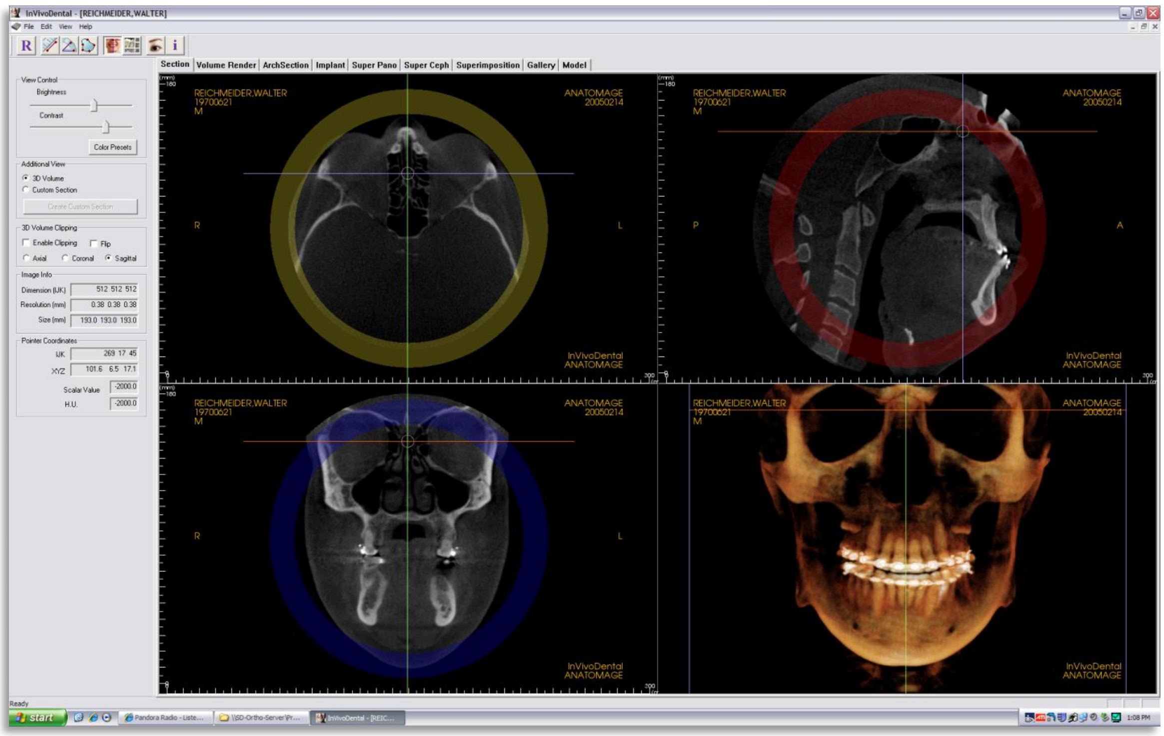


**Figure 4: A screen view of one patient depicted in three different planes in which the different colored circles provide a method to modify the orientation of the head using the Anatomage software.**

9. Define the coronal orientation plane (x-axis; Figure 5)
    a. Identify the zygomaticofrontal (ZF) sutures bilaterally (if ZF sutures are unavailable, use the infraorbital rim to define x-axis)
    b. Orient the plane to simultaneously bisect both sutures
    c. Confirm that the plane is satisfactory by referring to individual plane sections in all views

d. If the zygomaticofrontal sutures are unavailable in the scan, use the infraorbital rims

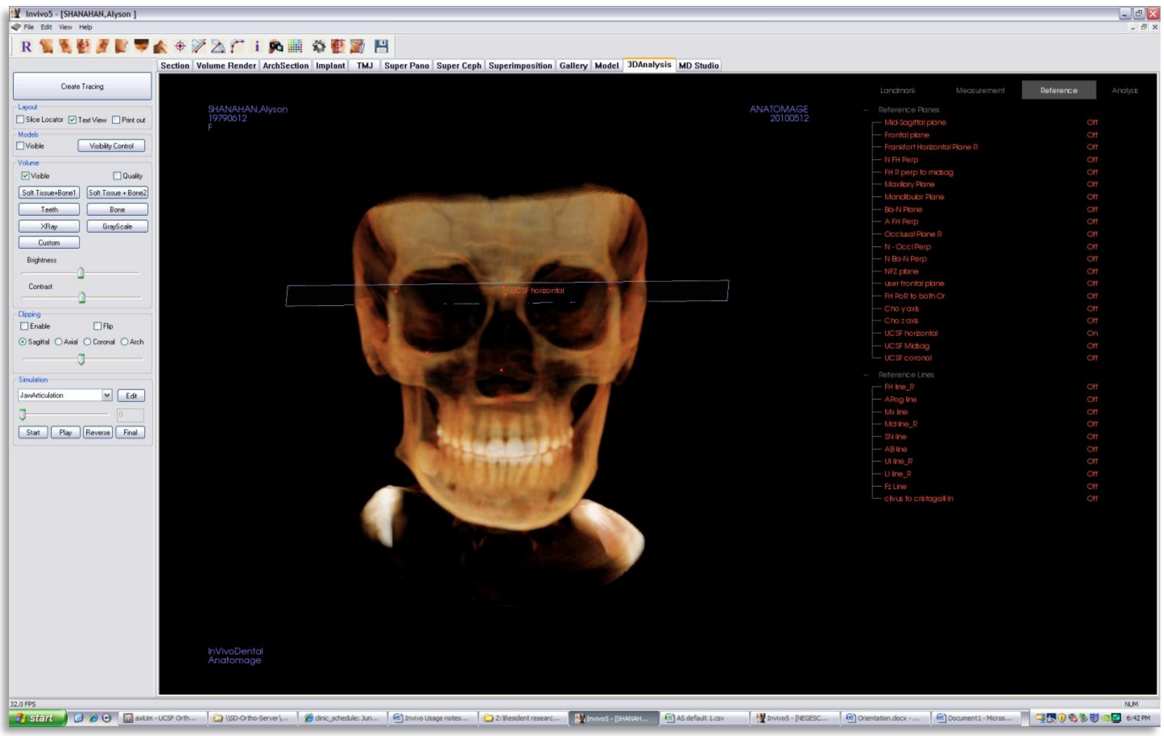


**Figure 5: Surface rendered volumetric view of one patient demonstrating the coronal orientation plane**

10. Define the axial orientation plane (y-axis; Figure 6)

    a. Identify crista galli (CG) using the sagittal and frontal sections

    b. Orient the plane to pass through Crista Galli superiorly in the frontal section

    c. Identify clivus (Cl) in the axial section

    d. Orient the plane to pass through Clivus inferiorly

e. Confirm that the plane is satisfactory by referring to individual sections in all views

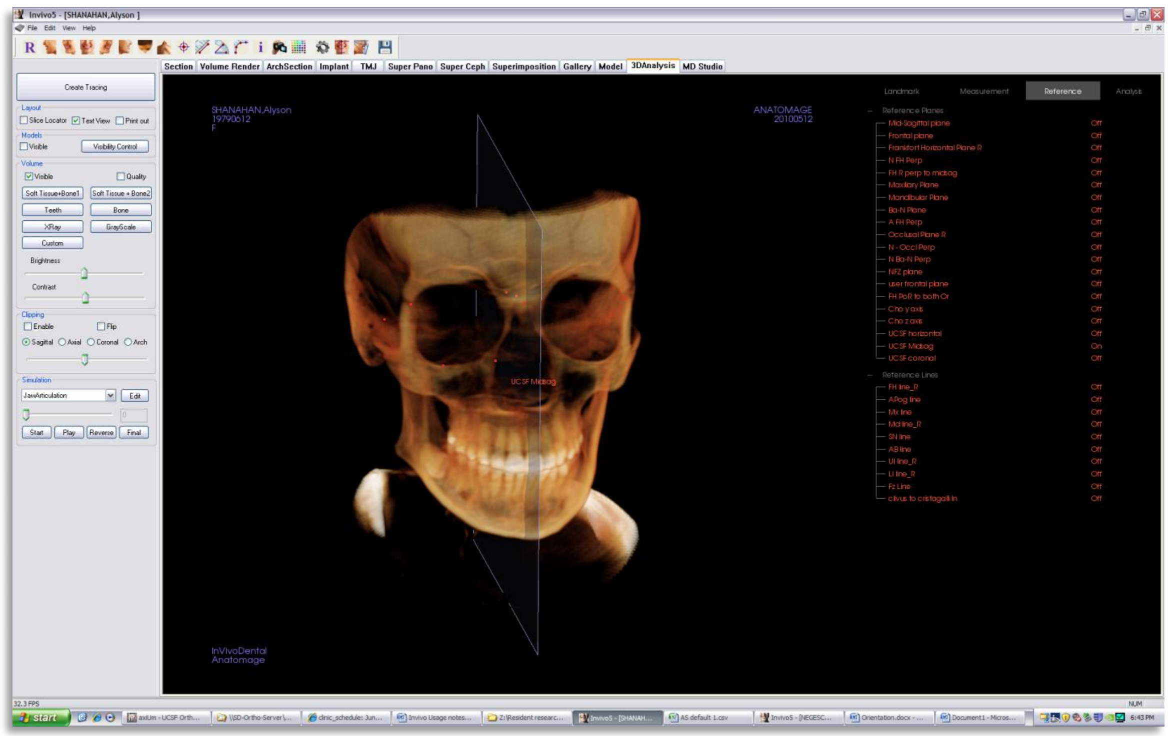


**Figure 6: Surface rendered volumetric view demonstrating the axial orientation plane**

11. Define the sagittal orientation plane (z-axis; Figure 7)

    f. Identify sella (S) in the sagittal section

    g. Identify nasion (N) in the sagittal section

    h. Orient the plane to pass through both sella and nasion simultaneously

    i. Confirm that the plane is satisfactory by referring to individual plane sections in all views

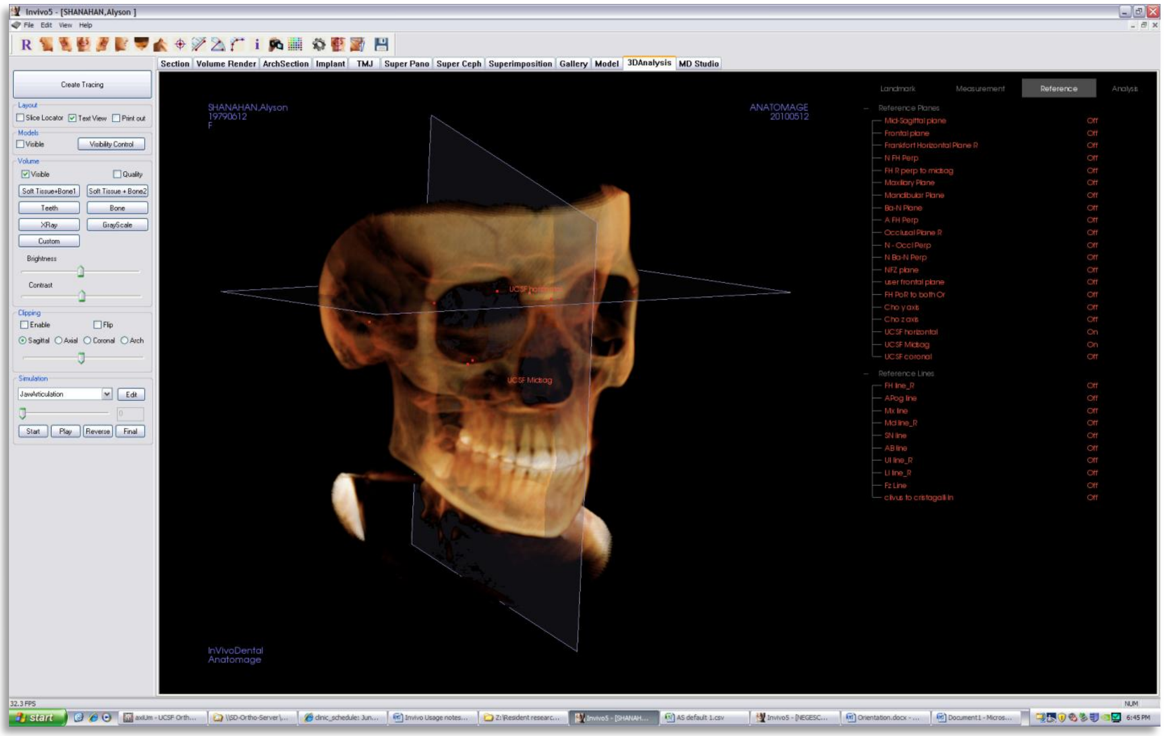

**Figure 7: Surface rendered volumetric view demonstrating the sagittal orientation plane**

12. Save orientation as a *.inv file

    a. Select “file” >> “save as”

    b. Select “*.inv” as the file type

    c. Click “Save”

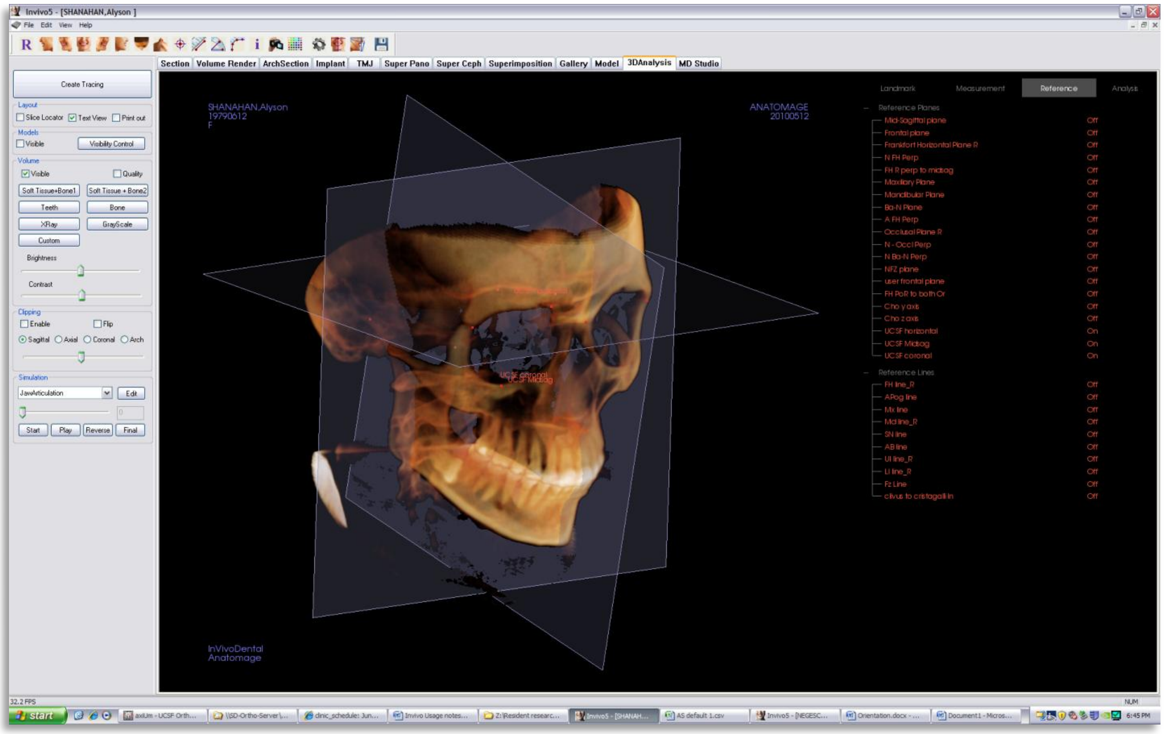


**Figure 8: Completed scan orientation based on coronal, axial and sagittal orientation planes**

## Reliability of Scan Orientation

Reliability of scan orientation was confirmed by measuring the three-dimensional distance between the origin of the scan, defined as point (0,0,0) to a pre-determined anatomical landmark using the formula: 3D distance = sqrt (x2 + y2 + z2). This measurement was obtained for each scan in a pilot group of 12 anonymized scans (4 subjects, 3 time-points per subject). This measurement was obtained on two occasions, three weeks apart. An Analysis of Variance was used for analysis, and a correlation coefficient was calculated, with R-squared equal to 0.98 (Harvey Kushner, Biostatistician, Biomedical Computer Research Institute Corp, Philadelphia, PA). The data are presented in Tables 1 and 2.

**Table 1: Coordinate points and calculated 3D distance from origin to Nasion (Reading 1)**

| Patient | | x | y | z | 3D distance |
|---|---|---|---|---|---|
| **1** | T0 | 0.06 | 23.8 | 17.8 | 29.7 |
| | T1 | 0.06 | 24.6 | 16.9 | 29.9 |
| | T2 | 0.67 | 23.5 | 18.8 | 30.1 |
| **2** | T0 | 2.37 | 16.6 | 11.2 | 20.1 |
| | T1 | -0.13 | 15.6 | 13.3 | 20.5 |
| | T2 | 2.90 | 15.3 | 10.9 | 19.1 |
| **3** | T0 | 0.26 | 13.5 | 10.5 | 17.1 |
| | T1 | 0.07 | 13.2 | 9.26 | 16.2 |
| | T2 | 0.16 | 12.6 | 10.5 | 16.4 |
| **4** | T0 | 0.83 | 20.8 | 4.60 | 21.3 |
| | T1 | -0.20 | 18.5 | 5.46 | 19.3 |
| | T2 | 1.58 | 19.1 | 4.22 | 19.6 |

**Table 2: Coordinate points and calculated 3D distance from origin to Nasion (Reading 2)**

| Patient | | x | y | z | 3D distance |
|---|---|---|---|---|---|
| **1** | T0 | 0.12 | 22.3 | 16.9 | 28.1 |
| | T1 | 0.09 | 23.3 | 16.8 | 28.7 |
| | T2 | 0.77 | 22.1 | 17.6 | 28.3 |
| **2** | T0 | 2.96 | 18.1 | 12.1 | 21.9 |
| | T1 | 0.93 | 16.6 | 14.3 | 21.9 |
| | T2 | 3.09 | 15.9 | 11.8 | 20.1 |
| **3** | T0 | 1.16 | 14.9 | 11.7 | 19.0 |
| | T1 | 0.87 | 14.0 | 7.90 | 16.2 |
| | T2 | 0.16 | 13.7 | 10.9 | 17.5 |
| **4** | T0 | 1.53 | 19.4 | 5.60 | 20.2 |
| | T1 | 0.25 | 19.1 | 6.05 | 20.1 |
| | T2 | 2.58 | 20.2 | 5.39 | 21.1 |

The method of orientation was shown to be reliable as there was a high correlation across all four subjects and all three time-points for the two reads with a final R-squared value of 0.98.

**Measurement Protocol**

A pilot group of four patients consisting of two Le Fort patients and two SARPE patients, selected at random, were used to design a measurement protocol. The patients each had a scan at three time-points (T0, T1, T2) for a total of twelve scans. The information was removed from the scans in order to mask the identity, time-point, and surgery type associated with each scan. After the scans were loaded into the software, twenty-six landmarks were identified bilaterally in order to formulate the measurements. The landmarks are presented in Table 3.

**Table 3: Definition of landmarks identified in Anatomage InVivo 5.x for pilot study (right and left)**

| | |
|---|---|
| **Maxillary first molar crown** | The most medial point of the maxillary first molar crown at the level of the furcation in the coronal plane and at the height of contour of the dental crown in the horizontal plane |
| **Maxillary first molar palatal root apex** | The apex of the palatal root of the maxillary first molar |
| **Maxillary first molar furcation** | The furcation of the maxillary first molar roots |
| **Maxillary first molar central fossa** | The central fossa of the occlusal surface of the maxillary first molar crown |
| **Maxillary canine** | The most medial point of the maxillary canine at the level of the height of contour in the horizontal plane |

| | |
|---|---|
| **Buccal cortical plate** | The lateral most point of the buccal cortical plate at the level of the furcation of the first molar in the coronal plane |
| **Incisive canal wall** | The wall of the incisive canal at the level of the root apices of the anterior dentition |
| **Greater palatine canal wall – superior (GPS)** | The inner wall of the greater palatine canal at the level of the nasal floor |
| **Greater palatine canal wall – Inferior (GPI)** | The point at which the inner wall of the greater palatine canal terminates and joins with the hard palate |
| **Lesser palatine canal wall – superior (LPS)** | The inner wall of the lesser palatine canal at the level of the nasal floor |
| **Lesser palatine canal wall – inferior (LPI)** | The point at which the inner wall of the lesser palatine canal terminates and joins with the hard palate |
| **Jugale (J-point)** | The radiographic point on the Jugal process at the intersection of the outline of the maxillary tuberosity and the zygomatic process |
| **Recess point of piriform rim** | A point on the piriform rim defined by bisecting an angle formed by two tangent lines to the base of the rim and the side of the rim. The recess point is defined as the point at which the bisecting line crosses the border of the aperture |

Based on these landmarks, twelve skeletal measurements were defined to quantify the changes in the posterior maxilla and the anterior maxilla. The greater and lesser palatine measurements were taken in two different views in the multiplanar reconstruction (axial and coronal) mode, and on two different levels superoinferiorly, due to the complex anatomy of the canal systems. After testing of the protocol and measurement reliability in the pilot group, one measurement was chosen (nasal floor and axial). The measurements are presented in Table 4.

**Table 4: Definition of skeletal measurements taken using Anatomage 5.x in pilot study**

| | |
|---|---|
| **Maxillary skeletal base** | Measured from Jugale-left to Jugale-right in the PA ceph rendering |
| **GP intercanal width – superior coronal view** | Measured from the left GPS to right GPS as viewed in the coronal section view |
| **GP intercanal width – inferior coronal view** | Measured from the left GPI to right GPI as viewed in the coronal section view |
| **GP intercanal width – superior axial view** | Measured from the left GPS to right GPS as viewed in the axial section view |
| **GP intercanal width – inferior axial view** | Measured from the left GPI to right GPI as viewed in the axial section view |
| **LP intercanal width – superior coronal view** | Measured from the left LPS to right LPS as viewed in the coronal section view |
| **LP intercanal width – inferior coronal view** | Measured from the left LPI to right LPI as viewed in the coronal section view |
| **LP intercanal width – superior axial view** | Measured from the left LPS to right LPS as viewed in the axial section view |
| **LP intercanal width – inferior axial view** | Measured from the left LPI to right LPI as viewed in the axial section view |
| **Incisive canal intracanal width – coronal view** | Measured from left inner wall to right inner wall at the level of the root apices of the anterior dentition in the coronal section view |
| **Incisive canal intracanal width – axial view** | Measured from left inner wall to right inner wall at the level of the root apices of the anterior dentition in the axial section view |
| **Piriform base width** | Measured from the left recess point to the right recess point of the piriform rim |

Based on the landmarks identified, six dentoalveolar measurements were defined. Three methods were used to define the angulation of the maxillary first molar using the landmarks previously defined. The measurements are presented in Table 5.

**Table 5: Definition of dentoalveolar measurements taken in Anatomage InVivo 5.x in pilot study**

| | |
|---|---|
| **Intermolar width** | Measured from the medial of the left maxillary first molar crown to medial of the right maxillary first molar crown |
| **Intercanine width** | Measured from the medial of the left maxillary canine crown to medial of the right maxillary canine crown |
| **Buccal alveolar width** | Measured from the lateral-most point of the buccal alveolar plate at the level of the furcation of the 1st molar, bilaterally |
| **Maxillary first molar angulation 1** | An angle formed by a line passing through the buccal cusp tip and the palatal root apex of the maxillary first molar and the horizontal reference plane |
| **Maxillary first molar angulation 2** | An angle formed by a line passing through the central fossa and the root furcation of the maxillary first molar and the horizontal reference plane |
| **Maxillary first molar angulation 3** | An angle formed by a line passing through the central fossa and the palatal root apex of the maxillary first molar and the horizontal reference plane |

To test our protocol and measurement reliability, we recruited two third-year UCSF dental students as research assistants to assist with the measurements and protocol testing. The research assistants were trained how to use the InVivo Anatomage software and were calibrated over three 2-3 hour sessions. Their understanding and competency were confirmed on the third session. They were instructed how to read the CBCT scans and how to make the required measurements based on the following measurement guideline:

## MEASUREMENT GUIDELINE

### Skeletal Measurements

**1. Maxillary base (Figures 9A and 9B)**

a. The Jugule (J-point) is defined as the point on the Jugal process at the intersection of the outline of the maxillary tuberosity and the zygomatic process

b. Draw a line extending from the left J-point to the right J-point

**c. Directions:**

i. Select the “super ceph” tab

ii. Click on the facial view preset

iii. Click “create ceph”

iv. Zoom in and take measurement

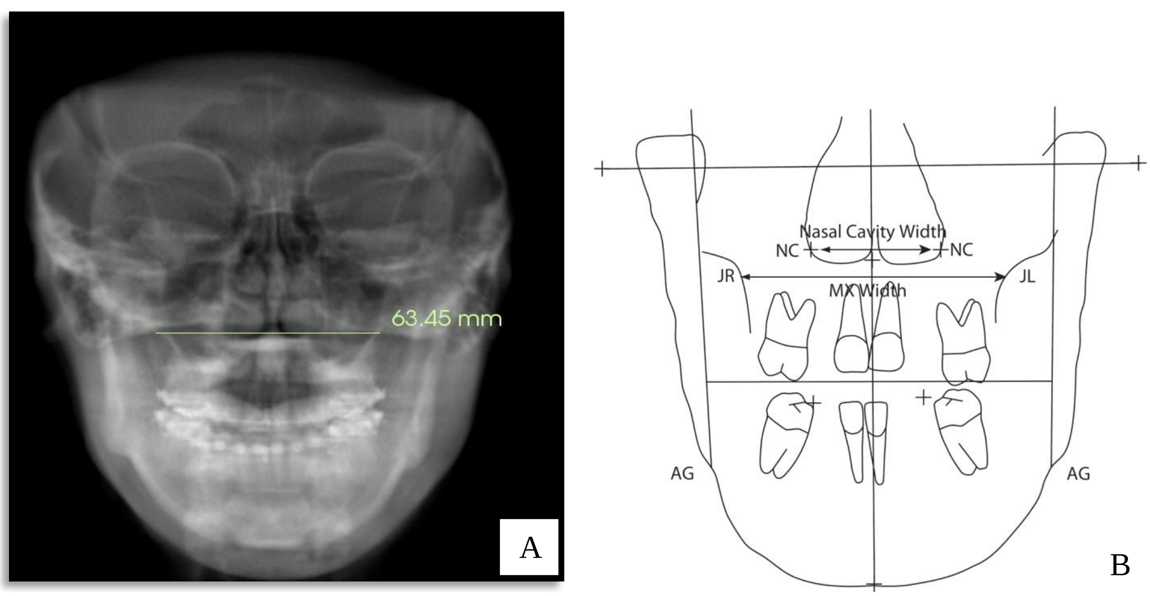


**Figure 9: A frontal full head x-ray of one patient (A) with a schematic of the frontal view indicating the landmarks and measurements (B).**

2. **Intercanal width – Greater palatine canal** (the greater palatine canal is located distal to the area of the 2$^{nd}$ molars on the sagittal slice and sometimes medial to the molars on the coronal slice, and can appear to be curved (**Figure 10)**

a. **Method 1 (Superior ):**

   i. Measured from the medial wall of the left greater palatine canal to the medial wall of the right greater palatine canal at the point at level of the nasal floor

   ii. Measurements taken using the axial section view and the coronal section view

b. **Directions:**

   i. Select “sections” tab

   ii. Zoom in on the maxilla in the axial section

   iii. Locate the greater palatine canals in the axial view with the scroll button under high contrast

   iv. Place the horizontal and sagittal reference planes (crosshairs) over the canal

   v. Set the horizontal reference plane at the level of the nasal floor in the coronal section

   vi. Use axial section to identify most posterior portion of the canal

vii. Make superior (nasal floor) measurement in the axial section view

viii. Repeat the measurement in the coronal section view at the level in which the horizontal reference plane is set coincident with the nasal floor.

**c. Method 2 (Inferior):**

i. Measured from the medial wall of the left greater palatine canal to the medial wall of the right greater palatine canal at the most posterior-inferior opening of the canal (point of exit)

ii. Measurement taken using the axial section view and the coronal section view

**d. Directions:**

i. Select the “sections” tab

ii. Zoom in on the maxilla in the axial section

iii. Locate the greater palatine canals in the axial view with the scroll button under high contrast

iv. Place the reference planes (crosshairs) over the canal

v. Use axial section to identify most posterior portion of the canal

vi. Use the coronal section to set the horizontal reference plane at the most inferior portion of the canal as it transitions into the hard palate

vii. Make inferior (point-of-exit) measurement in the axial and coronal sections

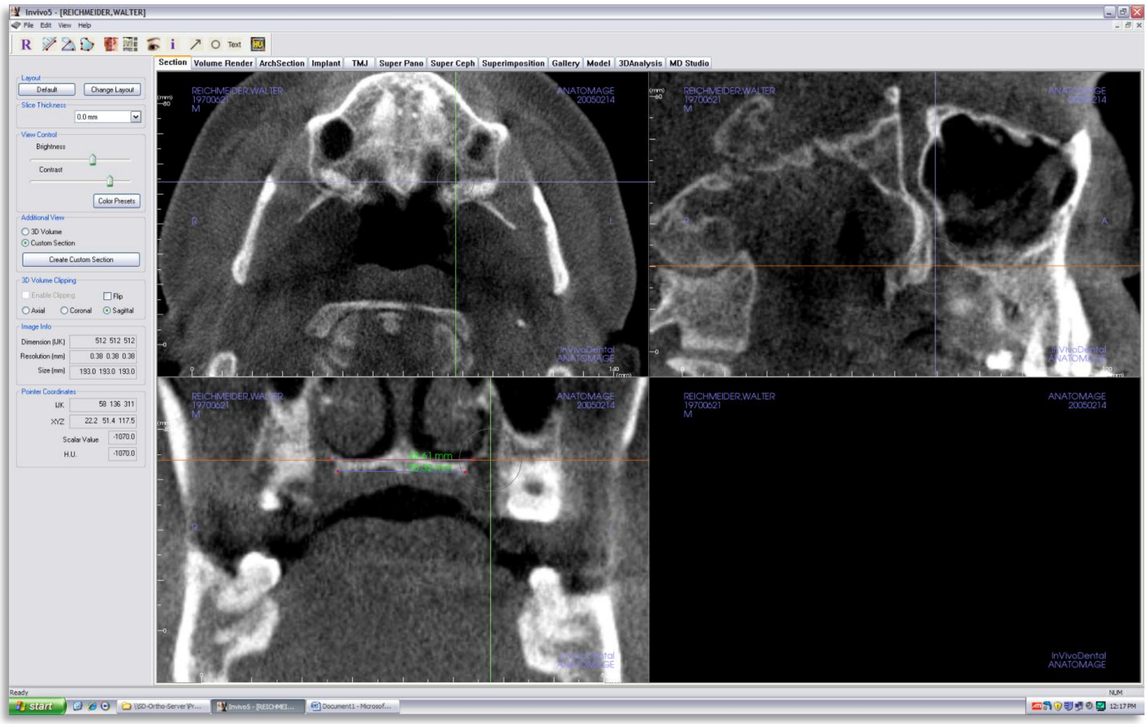

**Figure 10: Multiplanar view of the greater palatine canals and measurements made at the level of the nasal floor and point of exit.**

3. **Intercanal width – Lesser palatine canal** (the lesser palatine is immediately distal to the greater palatine canal and smaller (Figure 11)

**a. Method 1 (Superior):**

i. Measured from the medial wall of the left lesser palatine canal to the medial wall of the right lesser palatine canal at the point at level of the nasal floor

ii. Measurements taken using the axial section view and the coronal section view

**b. Directions:**

i. Select “sections” tab

ii. Zoom in on the maxilla in the axial section

iii. Locate the lesser palatine canals in the axial view with the scroll button under high contrast (the lesser palatine canals are circular and located directly posterior to the greater palatine canals; they often have a distinct cortical outline in the axial view)

iv. Place the horizontal and sagittal reference planes (crosshairs) over the canal

v. Set the horizontal reference plane at the level of the nasal floor in the coronal section

vi. Make superior (nasal floor) measurement in the axial section view

vii. Repeat the measurement in the coronal section view at the level in which the horizontal reference plane is set coincident with the nasal floor.

**c. Method 2 (Inferior):**

i. Measured from the medial wall of the left lesser palatine canal to the medial wall of the right lesser palatine canal at the most posterior-inferior opening of the canal (point of exit)

ii. Measurement taken using the axial section view and the coronal section view

**d. Directions:**

i. Select the “sections” tab

ii. Zoom in on the maxilla in the axial section

iii. Locate the lesser palatine canals in the axial view with the scroll button under high contrast

iv. Place the reference planes (crosshairs) over the canal

v. Use axial section to identify most posterior portion of the canal

vi. Use the coronal section to set the horizontal reference plane at the most inferior portion of the canal as it transitions into the hard palate

vii. Make inferior (point-of-exit) measurement in the axial and coronal sections

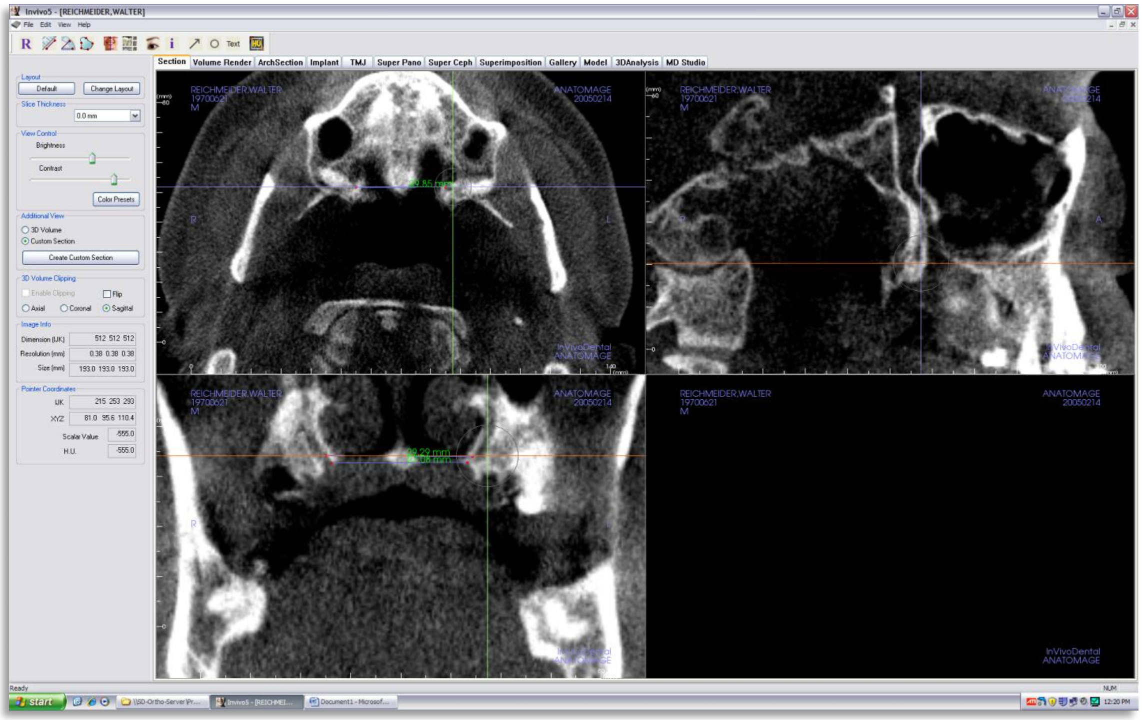


**Figure 11: Multiplanar view of the lesser palatine canals and measurements made at the level of the nasal floor and point of exit.**

**4. Incisive canal width (Figure 12)**

**a.** Measured from the axial section view and coronal section view

**b.** Draw a line extending from the left inner wall to the right inner wall of the incisive canal at the level of the root apices. The incisive canal is located lingual to the central incisors, often in line with the canines in the axial view.

**c. Directions:**

i. Locate the incisive canal on the axial view using the scroll button at high contrast

ii. Make 1st measurement in the axial view

iii. Place the crosshairs over the canal in the axial view

iv. Set the axial reference plane at the root tips on the sagittal view

v. Measure the intracanal distance on the coronal view at the level of the preset axial plane

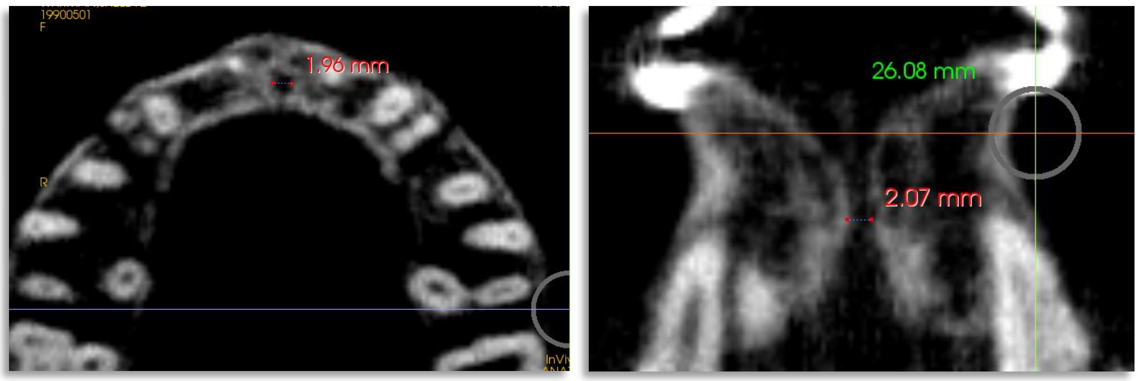


**Figure 12: Two different planes of view of the incisive canal (axial – left, coronal - right)**

**5. Piriform aperture base width (Figure 13)**

**a.** Measured in the volumetric rendering, this measurement uses tangent lines to the sides and base of the piriform aperture to construct reference points from which to define the base width of the inferior border.

**b. Directions**

**i.** Draw a line tangent to the left and right sides of the piriform aperture

**ii.** Draw a line tangent to the base of the piriform aperture

**iii.** The 3 lines drawn will form 2 angles at the base of the rim, angles P1 and P2

iv. Draw line L1 bisecting the angle P1 ; draw line L2 bisecting angle P2

v. The measurement is made at the point where L1 and L2 cross the edge of the piriform rim, which we will call the piriform recesses

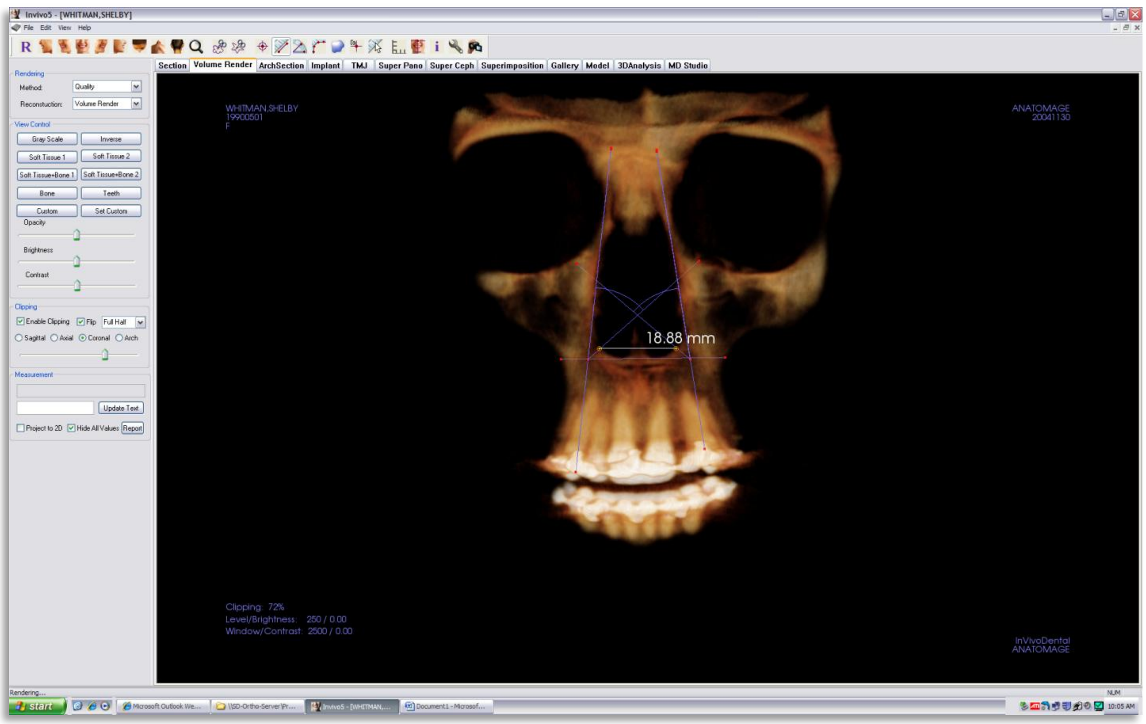


**Figure 13: Surface rendered volumetric view demonstrating construction of tangents and angles to measure the base width of the piriform aperture**

## Dentoalveolar measurements

### 6. Intermolar width (Figure 14)

**a.** Measured from the axial view at the level of the furcation of the first molar and the height of contour of the first molar crown, bilaterally

**b.** Measured on a line extending from the most-medial point of the left first molar to the most-medial point of the right first molar

**c. Directions:**

- **i.** Set the sagittal reference plane at the $1^{st}$ molar furcation
- **ii.** Set the axial reference plane at the height of contour of the $1^{st}$ molar (in the coronal plane view)
- **iii.** Zoom in and measure using the axial plane view

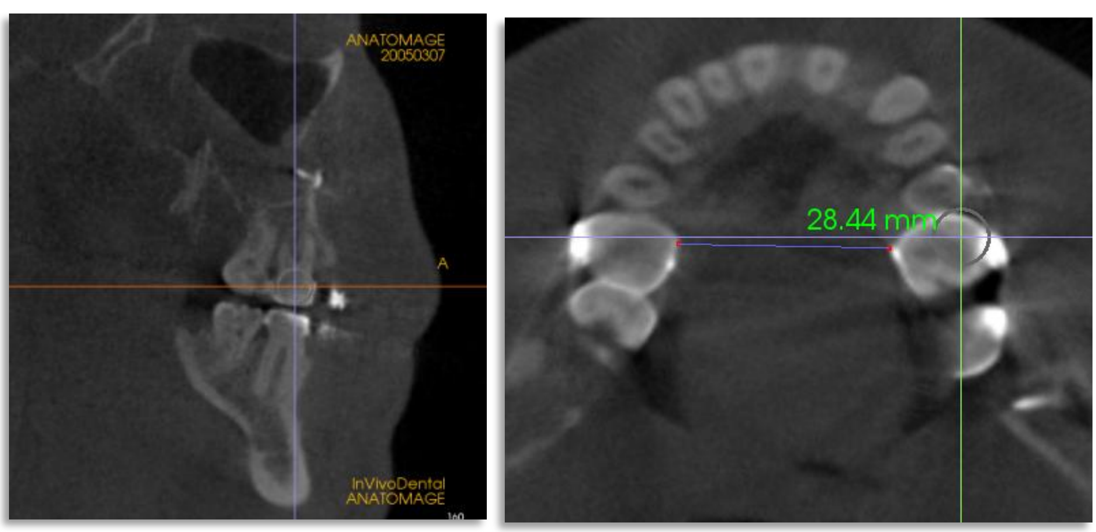


**Figure 14: Sagittal section view demonstrating identification of furcation of maxillary $1^{st}$ molar and height of contour (left) and axial section view demonstrating measurement of intermolar width (right)**

**7. Intercanine width (Figure 15)**

**a.** Measured from the axial view as confirmed using the sagittal slice

**b.** Draw a line extending from the most-lingual point of the left canine to the most-lingual point of the right canine

**c. Directions:**

**i.** Locate canine using crosshairs in the axial plane view

**ii.** Place axial reference plane at the height of contour of the canine (in the sagittal view)

**iii.** Measure the mesial-most point on the canine on the axial plane view, bilaterally

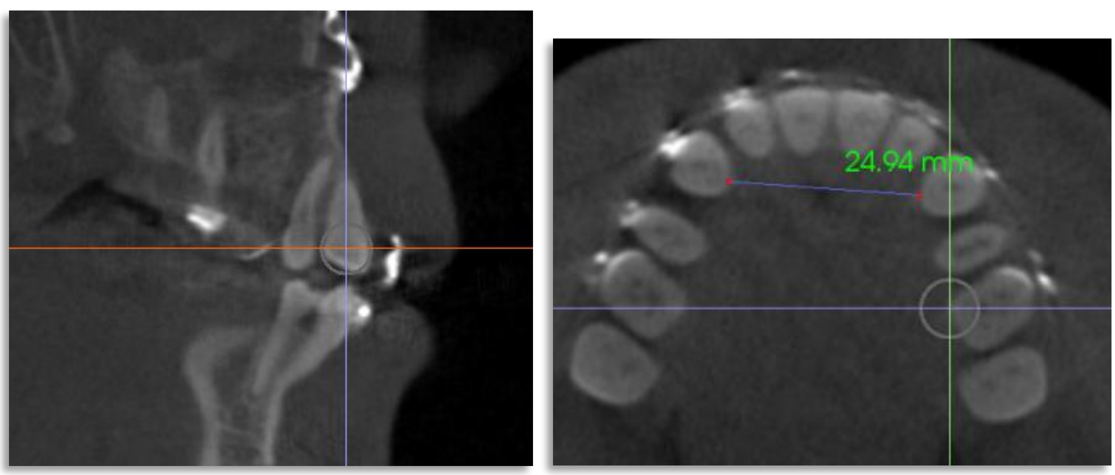


**Figure 15: Sagittal section view demonstrating identification of the maxillary canine height of contour (left) and axial section view demonstrating measurement of intercanine width (right)**

8. **Buccal cortical plate (Figure 16)**

a. Measured from the coronal view

b. Draw a line extending from the buccal-most point on the left alveolar cortical plate to the buccal-most point on the right alveolar cortical plate at the level of the furcation of the first molar as confirmed in the sagittal slice

c. The vertical reference line can be used as a reference tangent in the coronal view.

d. **Directions:**

   i. Locate the furcation of the 1st molar on the sagittal view

   ii. Measure from the buccal-most point on the alveolar process, bilaterally

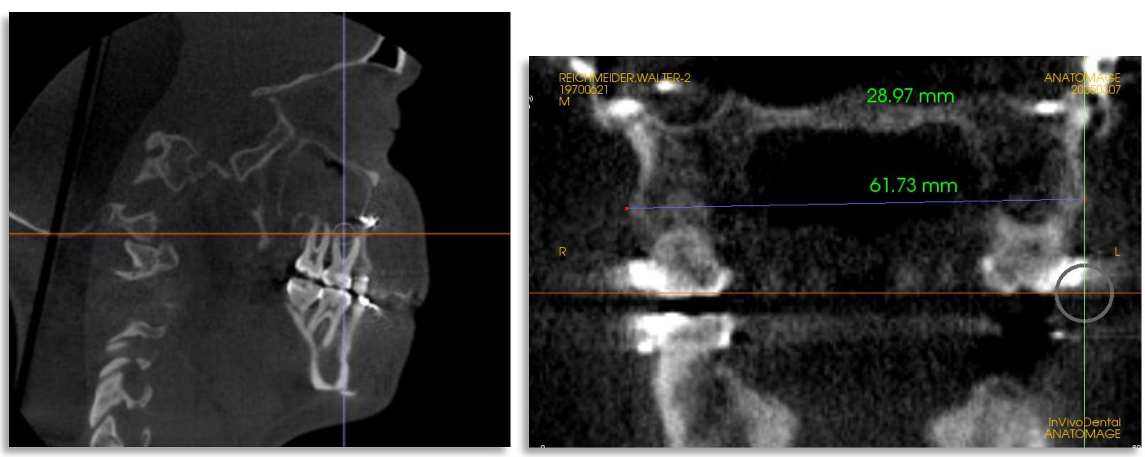


**Figure 16: Sagittal section view demonstrating identification of furcation of maxillary 1st molar (left) and axial section view demonstrating measurement of buccal cortical plate width (right)**

9. **Molar angulation (Figure 17-19)**

**a. Method 1:**

**i.** Locate the 1st molar palatal root in the axial view

**ii.** Set sagittal reference line through the palatal roots bilaterally in the axial view

**iii.** Measure the angle formed by a vertical line through the buccal cusp tip and the palatal root tip and the axial reference plane at high contrast; do this for both molars.

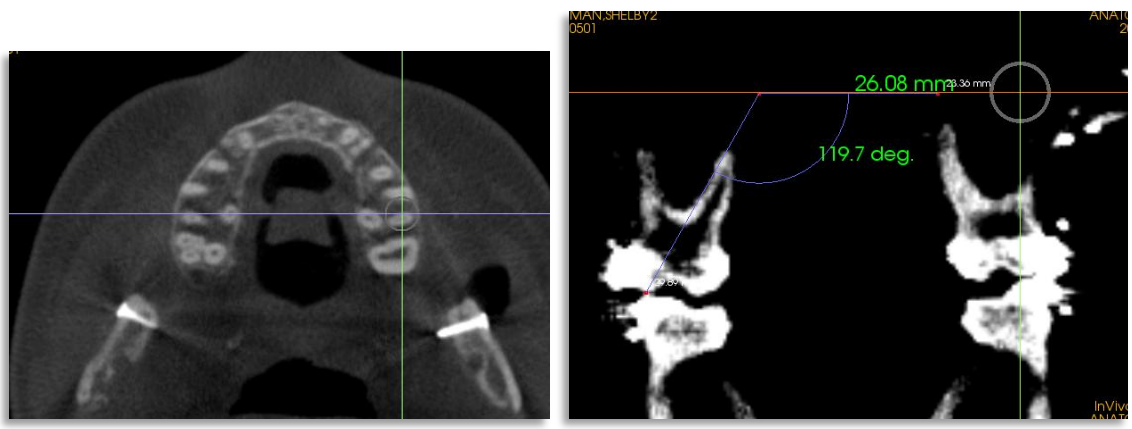


**Figure 17: Axial section view demonstrating location of sagittal and axial references (left) and coronal section view demonstrating 1st method of measuring molar angulation**

**a. Method 2:**

**i.** Measure the angle formed by a vertical line passing through the central fossa and the 1st molar furcation and the axial reference plane; do this for both molars

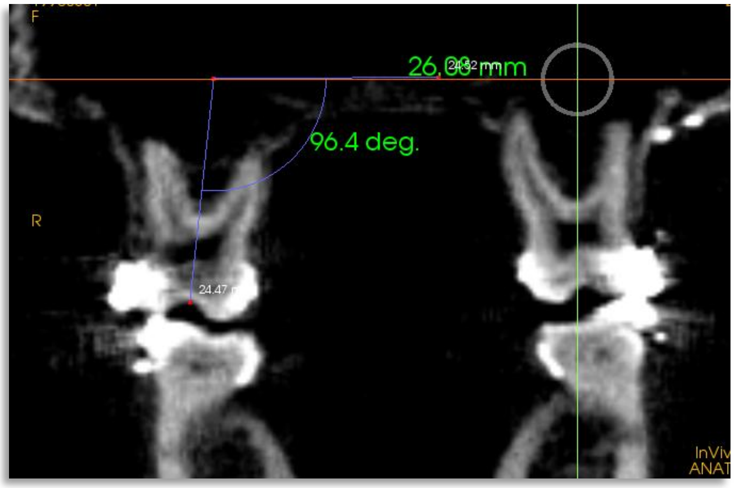


**Figure 18: Coronal section view demonstrating 2nd method of measuring molar angulation**

**b. Method 3:**

i. Measure the angle formed by a vertical line passing through the central fossa and the palatal root tip and the axial reference plane; do this for both molars

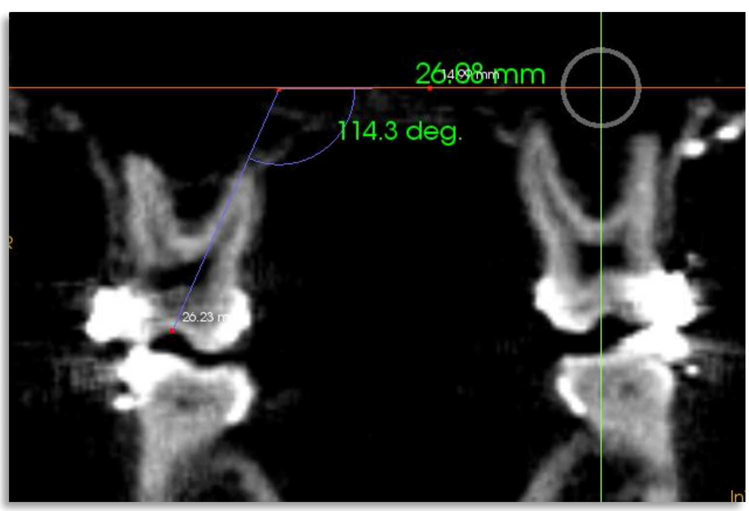


**Figure 19: Coronal section view demonstrating 3rd method of measuring molar angulation**

After completion of the pilot study and statistical analysis to determine measurement reliability, four measurements were selected to be used in the second part of the study. These measurements are the greater palatine canal at the level of the nasal floor as viewed from the axial section (representing the posterior skeletal width of the maxilla), the width of the base of the piriform aperture (representing the anterior skeletal width), the intermolar distance (representing the posterior dental measurement) and the intercanine distance (representing the anterior dental measurement). The data and statistical analysis of the pilot study will be presented in detail in the Results section of this paper.

**Part Two: Evaluating Skeletal and Dental Expansion and Relapse**

**Patient Selection**

This was a prospective longitudinal study approved by the University of California, San Francisco (UCSF) Committee on Human Research. A total of 13 patients (7 female, 6 male) were recruited for the study from the UCSF Orthodontic Clinic and UCSF Department of Oral and Maxillofacial Surgery. The authors of this study obtained informed consent. The patient selection criteria were as follows:

**Inclusion Criteria:**

1. Subjects diagnosed with skeletal maxillary transverse deficiency (MTD) requiring surgical expansion of the maxilla
2. Subjects undergoing a 2-piece or 3-piece segmental LeFort I Osteotomy or a Surgically Assisted Rapid Palatal Expansion (SARPE) to correct MTD
3. Subjects at the UCSF Oral and Maxillofacial Surgery Department
4. Subjects must have received cone beam computed tomography (CBCT) scans at 3 time points defined as follows:
    a. Le Fort (T0=preoperative, T1 = post-operative, T2 = 6+ months postoperative)
    b. SARPE (T0 = preoperative, T1 = post-expansion retention, T2 = 6+ months)

**Exclusion criteria:**

1. Patients missing the required set of CBCT scans
2. Patients with craniofacial anomalies that could alter the effects of expansion
3. Patients undergoing revision surgery

Enrollment for this study was open for approximately 24 months from August 2008 to August 2010. Subjects included in the study were assigned a number randomly to remove his/her identity. The subjects were categorized into

2 groups based on surgery type: 1) 2 or 3-piece segmental Le Fort I Osteotomy; and 2) SARPE. Eleven patients were recruited into the Le Fort group and seven patients were recruited into the SARPE group. A summary of the patient demographics for the final sample can be found in the following tables (Tables 6 and 7).

**Table 6: Patient Data for Le Fort Group**

| Patient | Gender | Age at Surgery (years) |
|---|---|---|
| 1 | F | 18.3 |
| 2 | M | 43.8 |
| 3 | F | 19.3 |
| 4 | F | 34.2 |
| 5 | F | 18.9 |
| 6 | M | 45.3 |
| 7 | M | 34.7 |
| 8 | M | 17.1 |
| 9 | M | 23.8 |
| | **4 female: 5 male** | **Avg = 28.4** |

**Table 7: Patient Data for SARPE Group**

| Patient | Gender | Age at Surgery (years) |
|---|---|---|
| 1 | F | 18.5 |
| 2 | M | 18.1 |
| 3 | F | 17.0 |
| 4 | F | 23.2 |
| | **3 female: 1 male** | **Avg = 19.2** |

## Surgical Protocols

### Segmental Le Fort I Osteotomy

All patients received pre-surgical orthodontics consisting of full fixed orthodontic appliances. A pre-surgical CBCT scan was taken (T0). Patients obtained maxillary transverse expansion guided by an intra-operative surgical splint. Stabilization of the segments was achieved via rigid fixation using titanium plates. Post-operative stabilization was determined by continuous use of a final surgical splint for 6 weeks with the support of elastic wear on surgical hooks. The surgical splints were made of acrylic resin using the model surgery technique on a fully adjustable dental articulator. The Department of Oral and Maxillofacial Surgery (OMFS) fabricated the splint prior to surgery, and surgery was performed in the Department. The surgical technique consisted of lateral maxillary osteotomies extending from the piriform aperture to the zygomatic buttress, bilaterally, and with a para-midsagittal cut along the middle palatine suture.

After the surgery, the patient returned for a post-operative CBCT scan (corresponding to time-point T1). The patient returned again for a third CBCT scan after 6 months (corresponding to time-point T2). The time intervals between T0, T1, and T2 are presented in Tables 8. The patient continued with full-fixed orthodontic treatment during this period and was monitored by OMFS with follow-up evaluations. After the data were obtained, it was analyzed using DICOM data in a 3D dental imaging software program (InVivo Anatomage 5.0, Anatomage, San Jose, California).

**Table 8: Time intervals between T0, Surgery, T1 and T2 in Le Fort Group**

| Patient | T0 – Surgery (days) | Surgery – T1 (days) | T1 – T2 (days) |
|---|---|---|---|
| 1 | 3 | 26 | 187 |
| 2 | 9 | 9 | 209 |
| 3 | 29 | 28 | 183 |
| 4 | 15 | 5 | 257 |
| 5 | 9 | 8 | 194 |
| 6 | 0 | 13 | 316 |
| 7 | 9 | 12 | 369 |
| 8 | 1 | 12 | 287 |
| 9 | 7 | 5 | 187 |
| | **Avg = 9 days** | **Avg = 13 days** | **Avg = 243 days** |

**Surgically assisted rapid maxillary expansion**

A pre-surgical CBCT scan was taken (T0). Subjects were fitted with a tooth-borne Hyrax expander prior to surgery. The expander consisted of an expansion screw with four 0.05-inch stainless steel arms soldered to four stainless steel bands fitted to the maxillary first premolars and molars (Figure 20). The expander is cemented in place using common light-cured glass ionomer cement and affixed to the maxillary first premolars and molars. A 0.036-inch stainless steel wire was placed lingual to the dentition to add rigidity and to extend the expansion to include the maxillary canines and second molars when present.

**Figure 20: Expansion appliance used for the SARPE patients**

Surgery was performed at the UCSF Department of Oral and Maxillofacial Surgery. The surgical technique consisted of all the surgical cuts involved in a bi-segmental Le Fort I Osteotomy and included bony separation at the pterygoid junction. Intraoperatively, the expansion appliance was activated to achieve a 1-2 mm separation at the maxillary central incisors. A latency period of one week was observed, after which patients were instructed to activate the expansion screw 0.25 mm twice a day (two turns per day). Patients were monitored weekly until the desired expansion was achieved. The expansion device was kept in place for a period of approximately 1 month until full fixed orthodontic brackets were bonded and orthodontic treatment was initiated on the maxillary teeth.

When expansion was complete, a CBCT scan was taken during the retention period (T1). The patient returned for a third scan after 6 months (T2). The time intervals between T0, expansion, T1, and T2 are presented in Table 9. After the data was obtained, it was be analyzed using Digital Imaging and Communications in Medicine (DICOM) data in a 3D dental imaging software program, Anatomage InVivo.

**Table 9: Time intervals in SARPE group**

| Patient | T0 – Surgery (days) | Expansion duration (days) | Post-expansion – T1 (days) | T1 – T2 (days) |
|---|---|---|---|---|
| 1 | 173 | 26 | 19 | 286 |
| 2 | 111 | 32 | 29 | 296 |
| 3 | 8 | 27 | 22 | 682 |
| 4 | 17 | 29 | 15 | 250 |
| | **Avg = 77** | **Avg = 28.5** | **Avg = 13** | **Avg = 243** |

**Cone Beam Computed Tomography**

A Hitachi CB MercuRay (Hitachi Medical Corporation, Tokyo, Japan) was used to obtain all patient scans. The machine was set to capture images at the manufacturer's recommended settings of 15-mA and 120-kVp. All patients were positioned in an upright, seated position, with their head stabilized against a headrest. During the scan, the patient was instructed to remain still, breathe through his/her nose, place his/her tongue at the roof of the mouth, and hold his/her teeth together in centric occlusion. The technician ensured that the scan was generated in natural head position by having the patient look into his or her own eyes in a mirror directly in front of the machine.

Each patient was scanned at three time-points: T0, T1, and T2. The first image (T0) was obtained prior to surgery in both the Le Fort group and the SARPE group. The second image (T1) was obtained after the surgery in the Le Fort group and after expansion in the SARPE group. The last image (T2) was obtained 6 months after completion of expansion. Isaacson showed that resistive forces that cause lateral changes in the alveolus are dissipated after 6 weeks post-expansion.[48] Bishara stated that the majority of healing after active expansion of the maxilla occurs within three months after expansion is completed.[30]

**Data analysis**

In the second part of the study, four measurements were used to evaluate the transverse skeletal and dentoalveolar changes in the maxilla as a result of surgical widening. The measurements are shown in Table 10.

**Table 10: Skeletal and dentoalveolar measurements**

| | |
|---|---|
| **Posterior dentoalveolar width** | Measured from the medial of the left maxillary first molar crown to medial of the right maxillary first molar crown |
| **Anterior dentoalveloar width** | Measured from the medial of the left maxillary canine crown to medial of the right maxillary canine crown |
| **Poterior skeletal width** | Measured from the most posterior point of the greater palatine canal in the axial view at the level of the nasal floor, bilaterally |
| **Anterior skeletal width** | Measured from the left recess point to the right recess point of the piriform rim |

**Table 11: Definition of ratios**

| | |
|---|---|
| **Percentage Expansion (%)** | mm expansion (T1-T0) / pre-surgical width at T0 |
| **Percentage Relapse (%)** | mm relapse (T2-T1) / post-expansion width at T1 |
| **Relapse rate (%)** | mm relapse (T2-T1) / mm expansion (T1-T0) |

## Statistical Analysis

The data from the pilot group was analyzed statistically to determine inter- and intra-reader reliability. Inter-reader reliability was evaluated using an Analysis of Variance with fixed effects and random effects. Intrareader reliablity was determined by calculating the coefficient of variation between the two reads and averaging over subjects, time-points and readers. The data from the pilot study and statistical analysis will be presented in the Results section.

A Wilcoxon signed-rank test was used to evaluate statistical significance of the reported outcomes values. A Wilcoxon two-sample rank-sum test was used to compare the ratio of dentoalveolar to skeletal change in the Le Fort and SARPE groups. All statistical analysis was performed using the SAS system (SAS systems, Cary, NC) with the help of Harvey Kushner (Biostatistician, Biomedical Computer Research Institute Corp, Philadelphia, PA).

## RESULTS

### Part One: Pilot Study

The raw data for the pilot study are presented in Figure 21. Inter-reader reliability is presented in Table 11. With respect to skeletal measurements in the maxilla, the greater and the lesser palatine canal were shown to be reliable for measuring width changes in the maxilla, however, only in the axial plane view, with $R^2$ values ranging from 0.82 to 0.92. Within this group, the measurements were more reliable when the horizontal level of the nasal floor was used as a reference, with $R^2$ = 0.87 and 0.92 for the greater and lesser palatine canal measurements, respectively. Measurements taken in the coronal plane view at the point-of-exit were not as reliable, with $R^2$ values ranging from 0.56 to 0.82. The piriform rim was a reliable measurement with an $R^2$ = 0.82. The maxillary base measurement was less reliable with an $R^2$ = 0.62. The incisive canal measurements were also less reliable with $R^2$ = 0.72 and 0.73. It is likely that the maxillary base and incisive canals are not reliable landmarks to use for measurement as they are areas of the anatomy that are intimately associated with the osteotomy site in both the LeFort procedure and the SARPE procedure. With respect to the dentoalveolar measurements, the intermolar distance and intercanine distance show average reliability with $R^2$ =0.76 and 0.79. The reliability of the molar angulation measures were low, ranging from $R^2$ = 0.49 to 0.61.

To measure intra-reader reliability, a coefficient of variation (C.V.) was calculated for each measurement, which expresses the variation as a percentage of the mean. The intra-reader reliability is presented in Table 12. All measurements demonstrated good to excellent intra-reader reliability, with the exception of the incisive canal measurements, with C.V. = 14.4 and 15.7.

With this information, two skeletal measurements and two dental measurements were selected to be used in the second part of the study. The skeletal measurements chosen were the GP axial – N to represent the posterior width of the maxilla, hereafter, referred to as “posterior skeletal”, and the piriform base width to represent the anterior width, hereafter, referred to as “anterior skeletal”. The dental measurements selected were the intermolar width to represent posterior dental change and the intercanine width to represent anterior dental change.

- **Skeletal Measurements**
  - Anterior – Base of the piriform aperture
  - Posterior – Greater palatine canal width (axial plane view, nasal floor)
- **Dental Measurements**
  - Intermolar width
  - Intercanine width

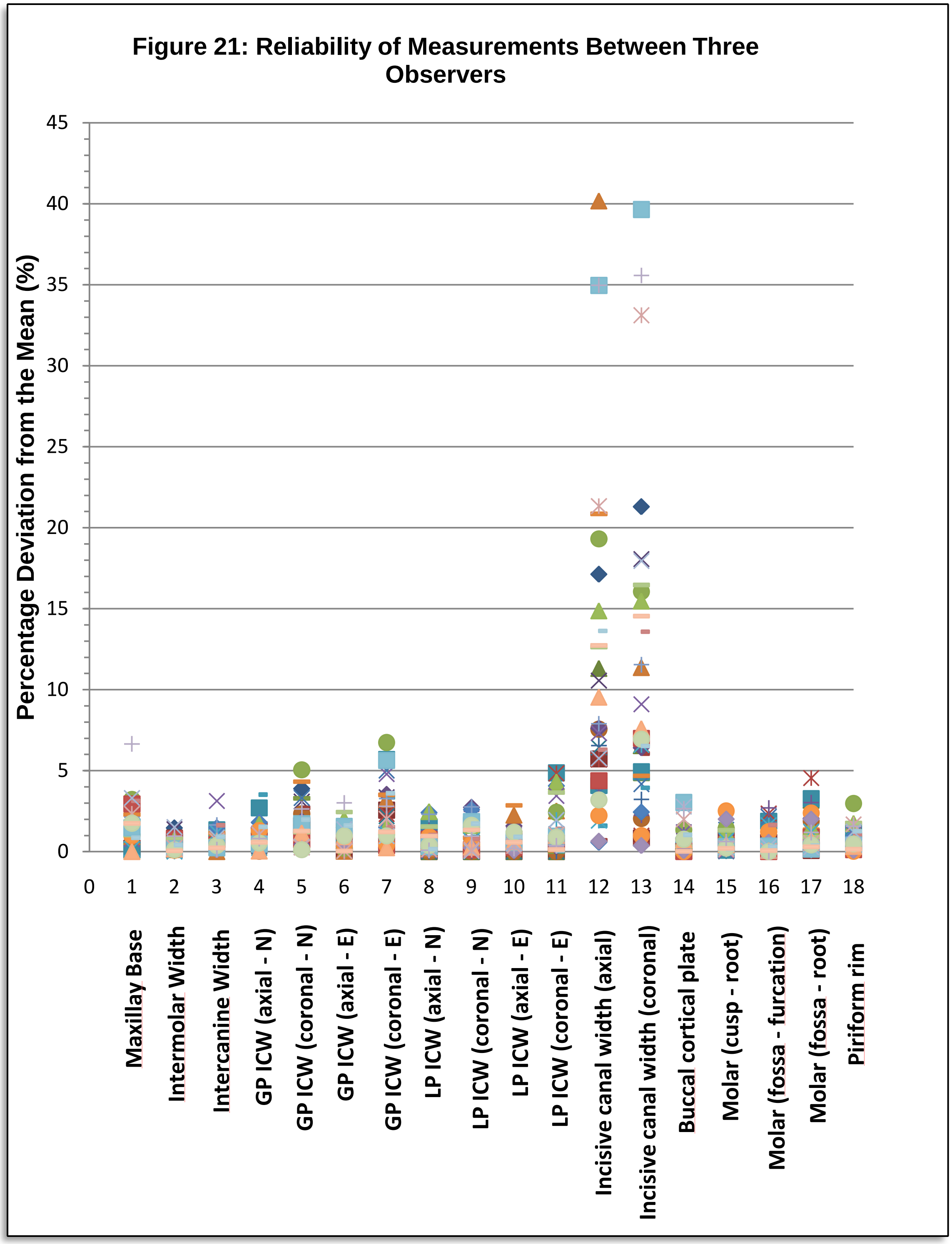


**Figure 21: Reliability of measurements between three observers plotted as percentage deviation from the mean. Individual color symbols represent each patient while the shape of the symbol represented the observer.**

**Table 12: Inter-reader Reliability**

| | R-Squared |
|---|---|
| **Maxillary Base** | 0.62 |
| **Intermolar Width (axial)** | 0.76 |
| **Intercanine Width (axial)** | 0.79 |
| **GP Intercanal width (axial - N)** | 0.87 |
| **GP Intercanal Width (coronal - N)** | 0.67 |
| **GP Intercanal width (axial - E)** | 0.82 |
| **GP Intercanal Width (coronal – E)** | 0.56 |
| **LP Intercanal Width (axial - N)** | 0.92 |
| **LP Intercanal Width (coronal - N)** | 0.90 |
| **LP Intercanal Width (axial - E)** | 0.87 |
| **LP Intercanal Width (coronal - E)** | 0.82 |
| **Incisive canal width (axial)** | 0.72 |
| **Incisive canal width (coronal)** | 0.73 |
| **Buccal cortical plate** | 0.80 |
| **Molar (cusp - root; R + L)** | 0.51 |
| **Molar (fossa - furcation; R + L)** | 0.61 |
| **Molar (fossa - root; R + L)** | 0.49 |
| **Piriform base width** | 0.82 |

**Table 13: Intra-reader Reliability**

| | Coefficient of variation (C.V.) |
|---|---|
| **Maxillary Base** | 1.26 |
| **Intermolar Width (axial)** | 0.76 |
| **Intercanine Width (axial)** | 1.28 |
| **GP Intercanal width (axial - N)** | 1.17 |
| **GP Intercanal Width (coronal - N)** | 2.00 |
| **GP Intercanal width (axial - E)** | 1.42 |
| **GP Intercanal Width (coronal – E)** | 2.71 |
| **LP Intercanal Width (axial - N)** | 1.08 |
| **LP Intercanal Width (coronal - N)** | 1.10 |
| **LP Intercanal Width (axial - E)** | 1.31 |
| **LP Intercanal Width (coronal - E)** | 1.75 |

| | |
|---|---|
| **Incisive canal width (axial)** | 15.4 |
| **Incisive canal width (coronal)** | 14.7 |
| **Buccal cortical plate** | 0.83 |
| **Molar (cusp - root; R + L)** | 0.88 |
| **Molar (fossa - furcation; R + L)** | 1.57 |
| **Molar (fossa - root; R + L)** | 1.91 |
| **Piriform base width** | 1.92 |

**Part Two:**

**Absolute skeletal changes in the Le Fort and SARPE groups**

All subjects showed an increase in posterior skeletal width from T0 to T1 (Figure 22). The Le Fort group had a mean expansion of 3.43 ± 1.24 mm ($p<.0005$). The SARPE group had a mean expansion of 0.50 ± 0.24 mm ($p<.05$). From T1 to T2, the Le Fort group had a mean relapse of 0.86 ± 0.42mm ($p<.0005$). From T1 to T2, the SARPE group had a mean increase in posterior skeletal width of 0.80 ± 0.54 mm, however, this change was not statistically significant (N.S.).

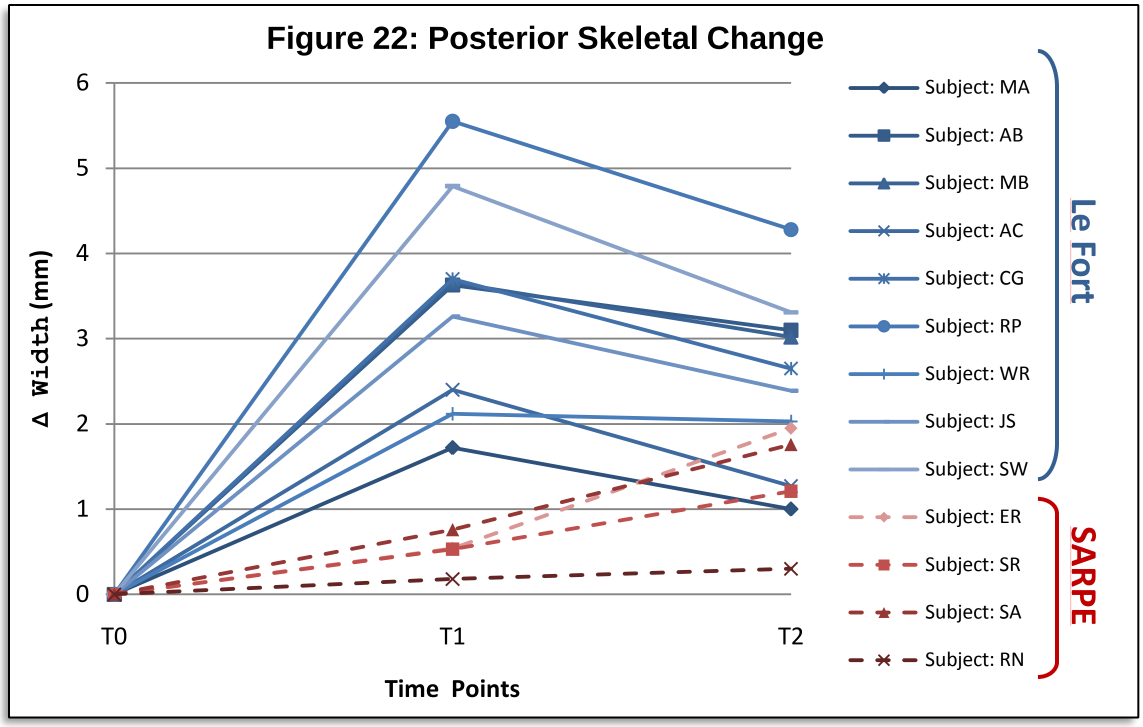


**Figure 22: Posterior skeletal change of SARPE and Le Fort Groups compared at three time-points, before surgery (T0), within one month post-expansion (T1), and at least six months after surgery (T2)**

Anteriorly, all subjects showed an increase in width from T0 to T2 (Figure 23). There was greater variation in the amount of expansion and relapse in the anterior maxilla when compared to the posterior maxilla. The Le Fort group had a mean increase of 1.94 ± 0.93 mm ($p<.0005$). The SARPE group had a mean increase of 2.25 ± 1.79 mm (N.S.). From T1 to T2, the Le Fort group showed a mean relapse of 0.55 ± 0.55 mm ($p<.05$) in anterior skeletal width. The SARPE group had an anterior skeletal relapse of 0.74 ± 0.63 mm (N.S.).

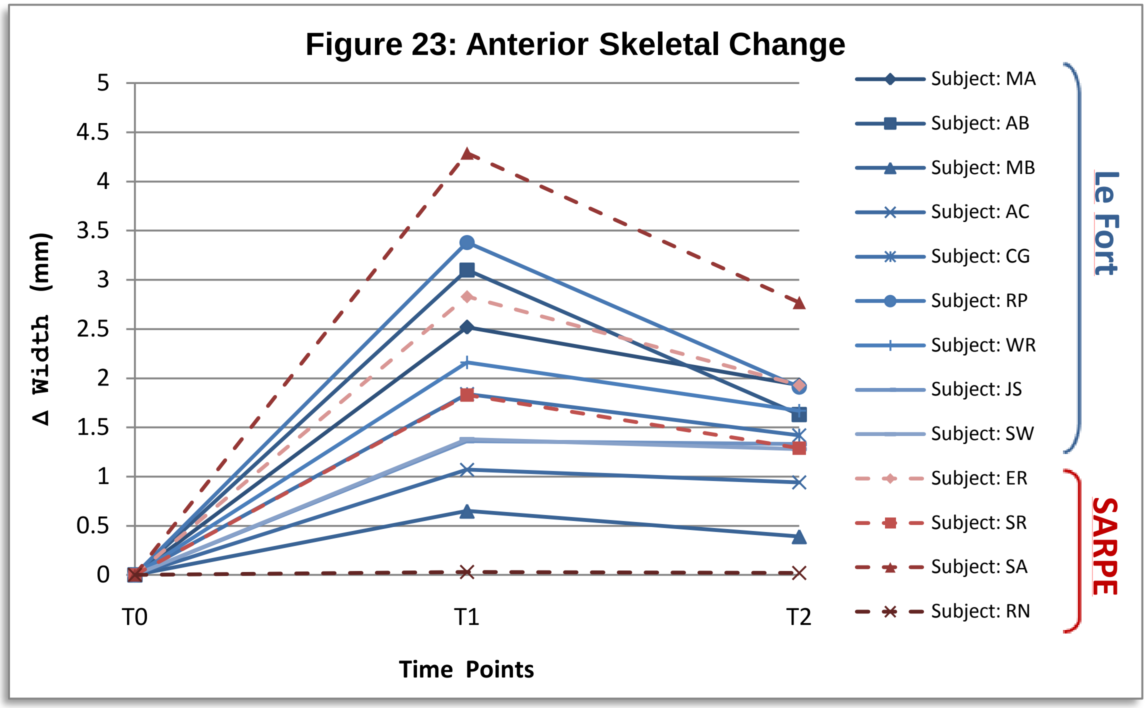


**Figure 23: Anterior skeletal change of SARPE and Le Fort Groups compared at three time-points, before surgery (T0), within one month post-expansion (T1), and at least six months after surgery (T2)**

### Absolute dental changes in the Le Fort and SARPE groups

Dentally, the Le Fort group demonstrated a mean increase of 2.17 ± 0.90 mm ($p<.0005$) at the molars and a mean increase of 1.01 ± 0.68 mm ($p<.005$) at the canines from T0 to T1. The SARPE group showed a significantly greater amount of dental expansion, with a mean increase of 10.0 ± 1.40 mm ($p<.0005$) at the molars, and mean increase of 5.33 ± 2.42 mm ($p<.05$) at the canines from T0 to T1. (Figures 24 and 25)

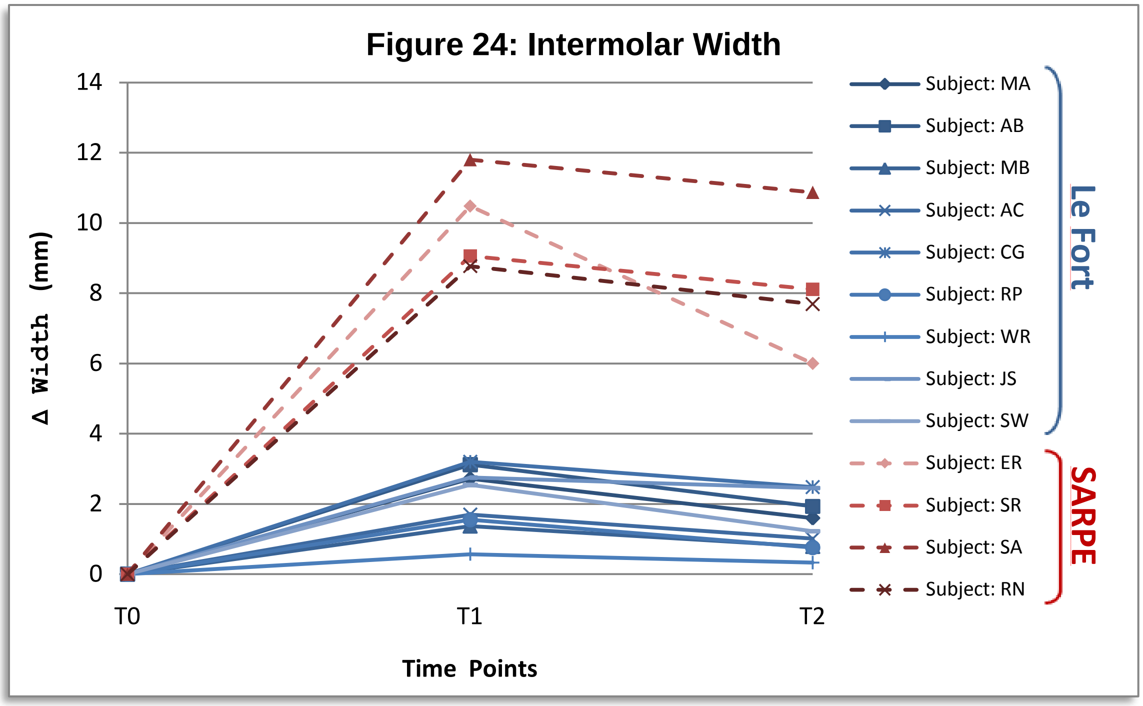


**Figure 24: Intermolar width change of SARPE and Le Fort Groups compared at three time-points, before surgery (T0), within one month post-expansion (T1), and at least six months after surgery (T2)**

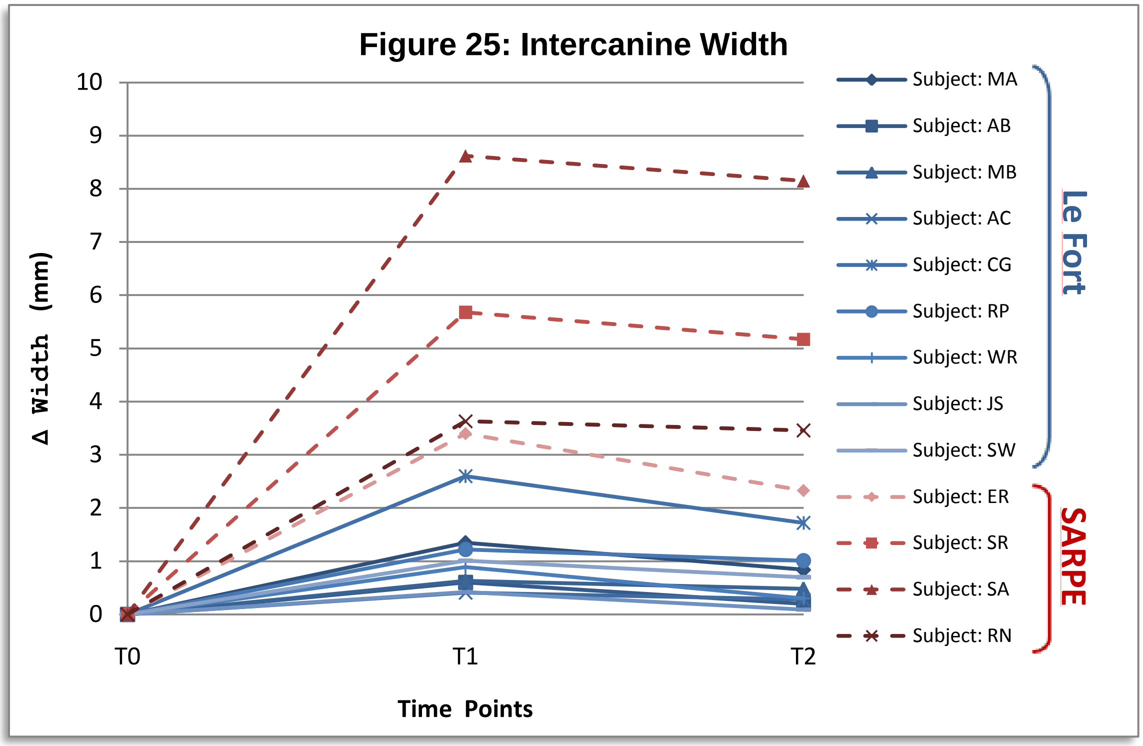


**Figure 25: Intercanine width change of SARPE and Le Fort Groups compared at three time-points, before surgery (T0), within one month post-expansion (T1), and at least six months after surgery (T2)**

From T1 to T2, the Le Fort group showed a mean dental relapse of 0.77 ± 0.38 mm (p<.0005) at the molars and 0.39 ± 0.24 mm (p<.005) at the canines. In the SARPE group, there was a mean relapse of 1.86 ± 1.75 mm (N.S.) at the molars and 0.56 ± 0.38 mm (N.S.) at the canines. The mean relapse observed in the SARPE group was not statistically significant.

Figures 26 and 27 summarize the absolute changes that occurred between time-points T0, T1 and T2 in both the Le Fort and SARPE groups.

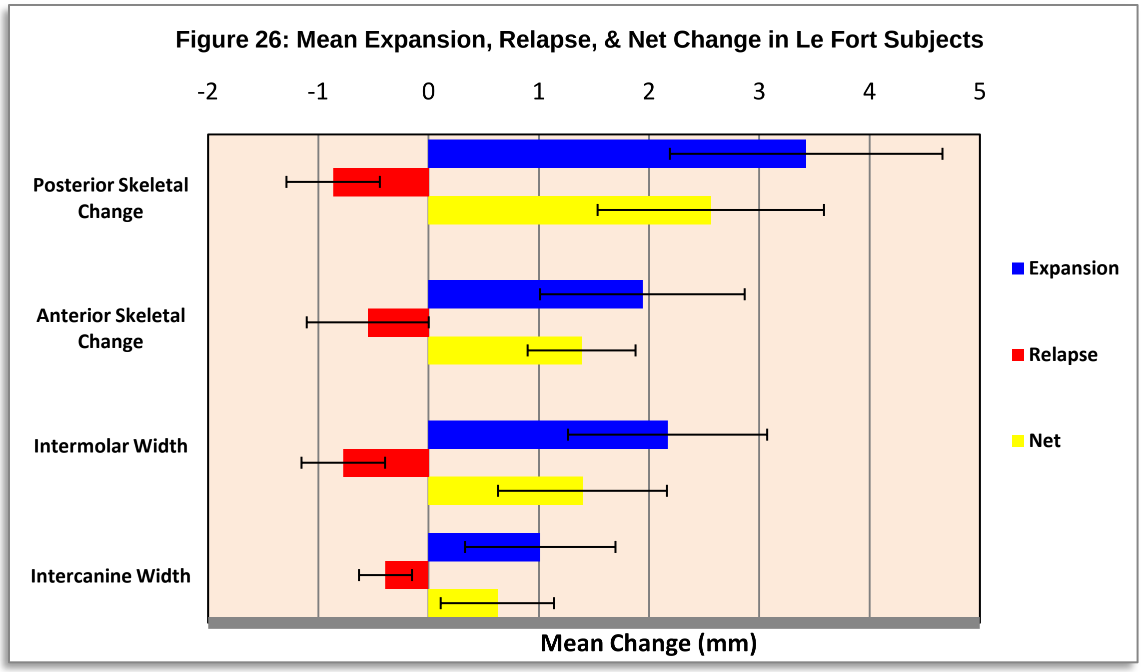


**Figure 26: Mean expansion, relapse and net change in LeFort subjects determined over the three time points.**

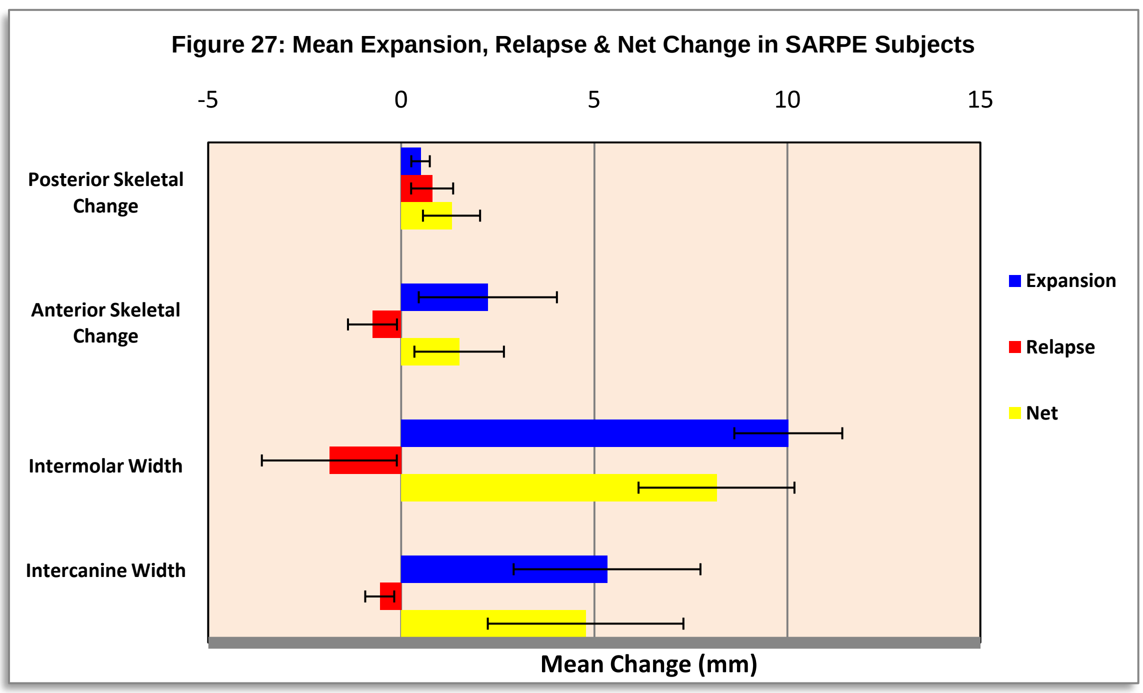


**Figure 27: Mean expansion, relapse and net change in SARPE subjects determined over the three time points.**

**Relative Expansion and Relapse: Le Fort Group**

The mean relative expansion in the Le Fort group is shown in Figure 28. Skeletally, the posterior width expanded 11.6 ± 4.30 % (p<.0005) and the anterior width expanded 9.95 ± 5.01 % (p<.0005). Dentally, the intermolar width had a relative expansion of 6.76 ± 2.98 % (p<.0005) and the intercanine width expanded 4.44 ± 3.30 % (p<.005).

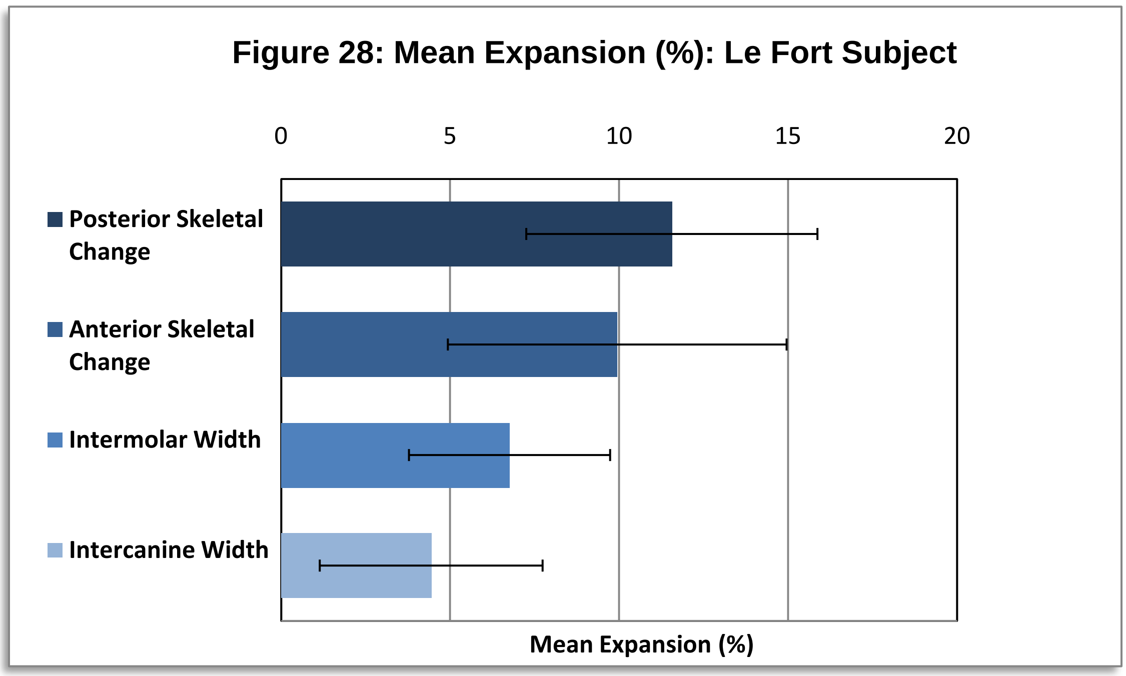


**Figure 28: Mean expansion in % for Le Fort Subjects at different segments**

The mean relative relapse in the Le Fort group is shown in Figure 29. Skeletally, the posterior width had a mean relative relapse of 2.61 ± 1.20 % (p<.0005) and the anterior width had a mean relative relapse of 2.51 ± 2.54 % (p<.05). Dentally, the intermolar width had a mean relative relapse of 2.25 ± 1.13

% (p<.0005) and the intercanine width had a mean relative relapse of 1.60 ± 1.01 % (p<.005).

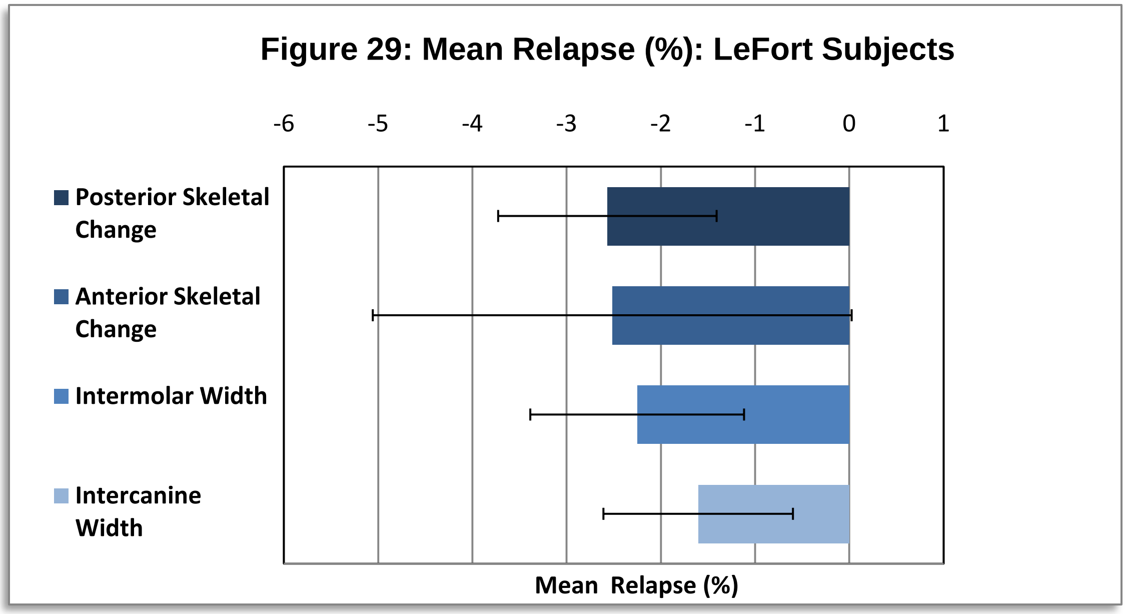


**Figure 29: Mean relapse in % for Le Fort Subjects at different segments**

The mean relapse rates in the Le Fort group are shown in Figure 30. Skeletally, the posterior width had a relapse rate of 26.0 ± 13.3 % (p<.0005) and the anterior width had a relapse rate of 24.6 ± 16.1 % (p<.005). Dentally, the intermolar width had a relapse rate of 37.9 ± 13.2 % (p<.0005) and the intercanine width had a relapse rate of 43.0 ± 21.8 % (p<.005).

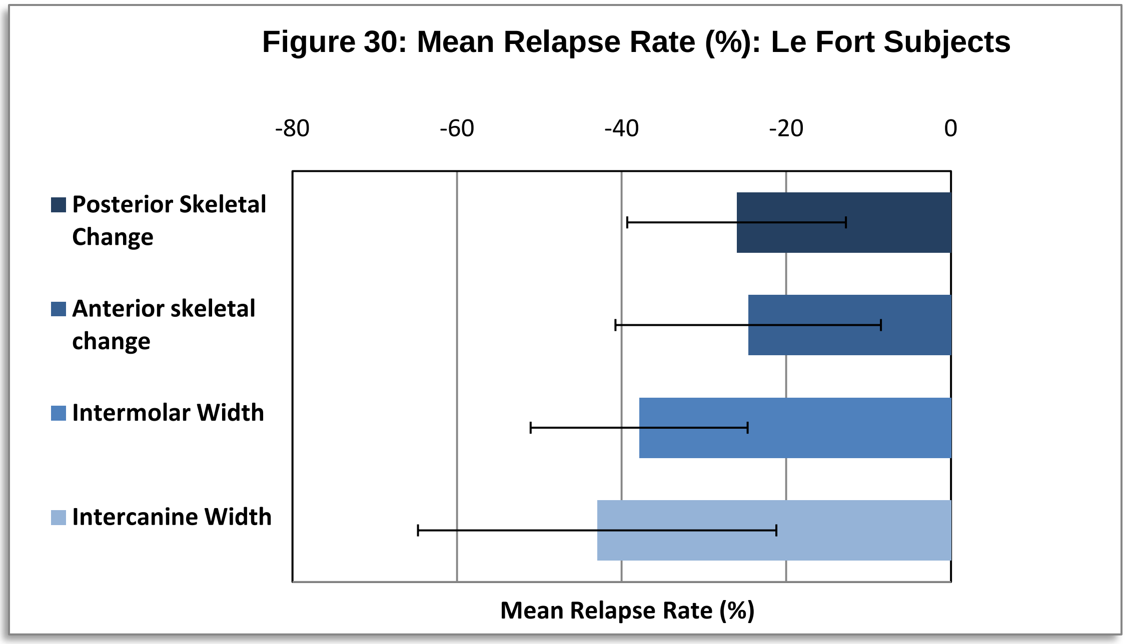


**Figure 30: Mean relapse rate in % for Le Fort Subjects at different segments**

## Relative Expansion and Relapse: SARPE Group

The mean relative expansion in the SARPE group is shown in Figure 31. Skeletally, the posterior width expanded 1.71 ± 0.82 % ($p<.05$) and the anterior width expanded 10.2 ± 7.71 % (N.S.). Dentally, the intermolar width had a relative expansion of 35.7 ± 8.39 % ($p<.005$) and the intercanine width expanded 28.6 ± 17.6 % ($p<.05$).

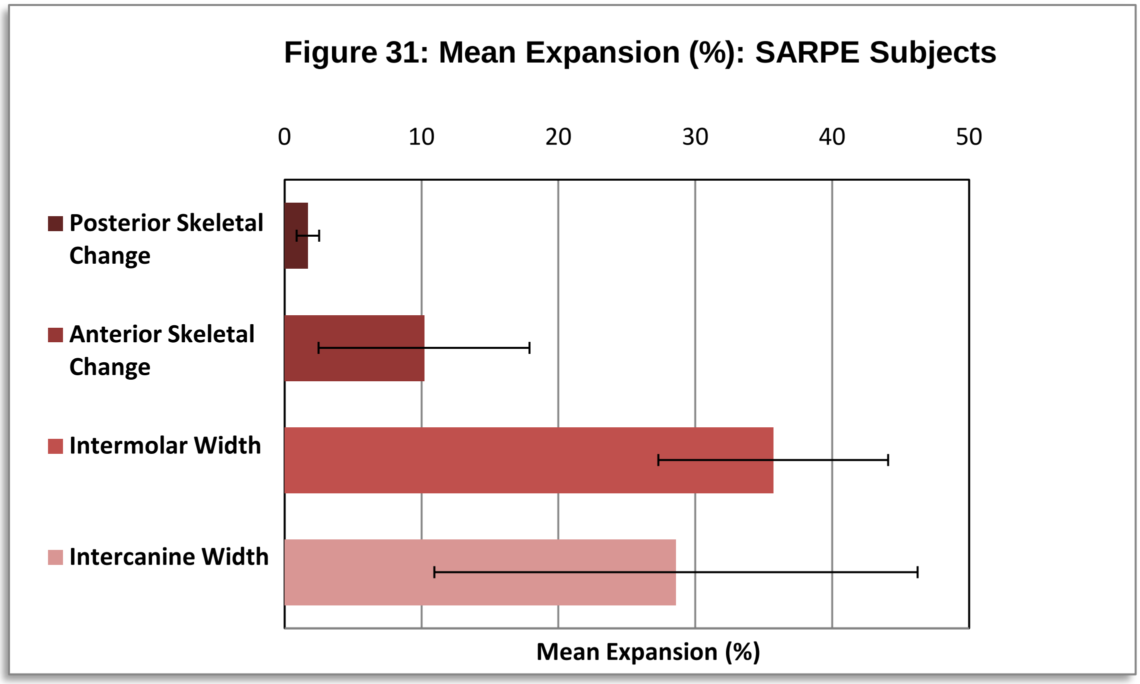


**Figure 31: Mean expansion in % for SARPE Subjects at different segments**

The mean relative relapse in the SARPE group is shown in Figure 32. Skeletally, the posterior width did not relapse, but continued to increase in width by 2.71 ± 1.90 % (N.S.); the anterior width had a mean relative relapse of 2.93 ± 2.29 % (N.S.). Dentally, the intermolar width had a mean relative relapse of 4.81 ± 4.51 % (N.S.) and the intercanine width had a mean relative relapse of 2.26 ± 1.64 % (N.S.).

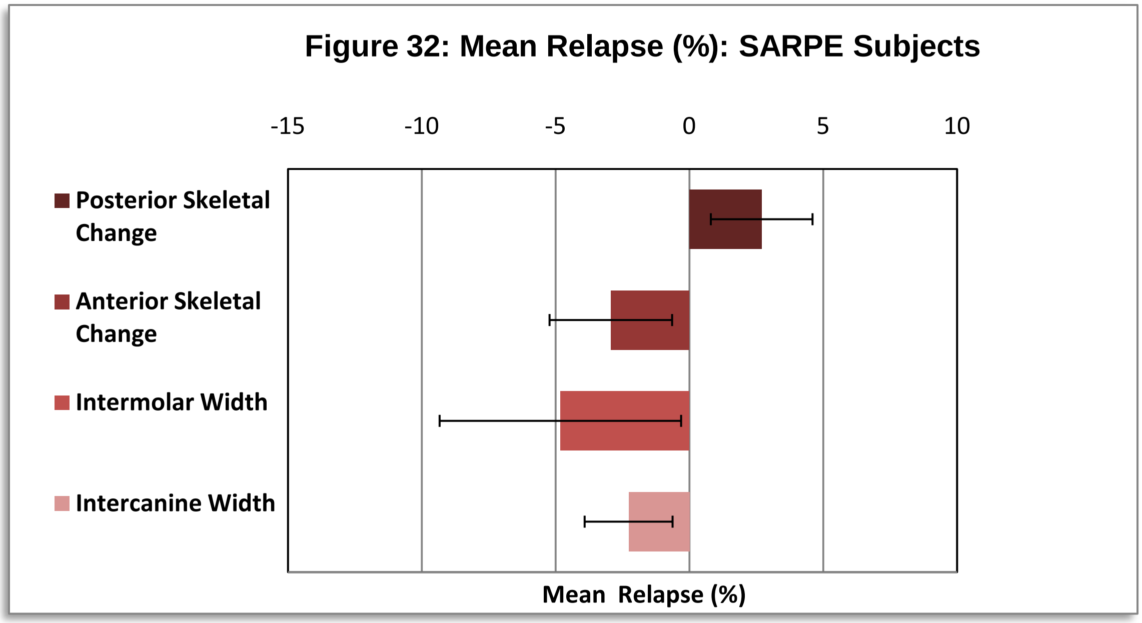


**Figure 32: Mean relapse in % for SARPE Subjects at different segments**

The mean relapse rates in the SARPE group are shown in Figure 33. Skeletally, the posterior width did not relapse, but expanded by 149.9 ± 81.7 % (p<.05); the anterior width had a relapse rate of 32.5 ± 32.5% (p<.0005). Dentally, the intermolar width had a relapse rate of 18.4 ± 16.4 % (N.S.) and the intercanine width had a relapse rate of 12.7 ± 12.7 % (N.S.).

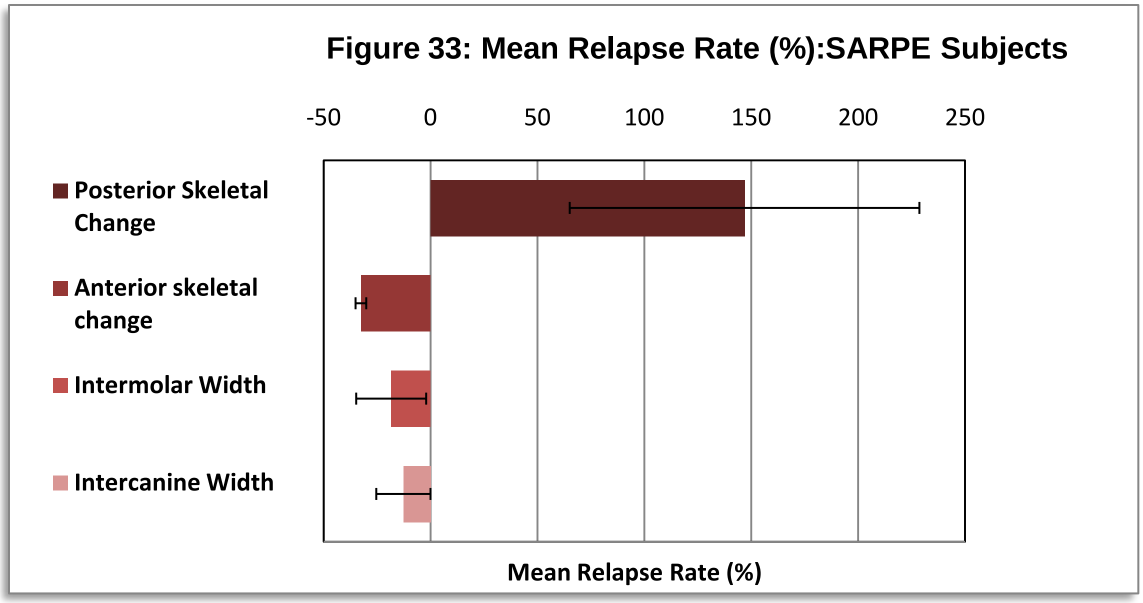


**Figure 33: Mean relapse rate in % for SARPE Subjects at different segments**

Absolute and relative changes in the Le Fort and SARPE groups are presented in Tables 14 and 15, respectively.

**Table 14: Summary of width changes in Le Fort group**

| | Mean Expansion | | P | Mean Relapse | | P |
|---|---|---|---|---|---|---|
| **Posterior Skeletal Change** | Absolute (mm) | 3.43 ± 1.24 | *** | Absolute (mm) | -0.86 ± 0.42 | *** |
| | Relative Expansion (%) | 11.57 ± 4.31 | *** | Relative Relapse (%) | -2.57 ± 1.16 | *** |
| | | | | Relapse Rate (%) | -26.0 ± 13.3 | *** |
| **Anterior Skeletal Change** | Absolute (mm) | 1.94 ± 0.93 | *** | Absolute (mm) | -0.55 ± 0.55 | * |
| | Relative Expansion (%) | 9.95 ± 5.01 | *** | Relative Relapse (%) | -2.51 ± 2.54 | * |
| | | | | Relapse Rate (%) | -24.6 ± 16.1 | ** |
| **Intermolar Width** | Absolute (mm) | 2.17 ± 0.90 | *** | Absolute (mm) | -0.77 ± 0.38 | *** |
| | Relative Expansion (%) | 6.76 ± 2.98 | *** | Relative Relapse (%) | -2.25 ± 1.13 | *** |
| | | | | Relapse Rate (%) | -37.9 ± 13.2 | *** |
| **Intercanine Width** | Absolute (mm) | 1.01 ± 0.68 | ** | Absolute (mm) | -0.39 ± 0.24 | ** |
| | Relative Expansion (%) | 4.44 ± 3.30 | ** | Relative Relapse (%) | -1.60 ± 1.01 | ** |
| | | | | Relapse Rate (%) | -43.0 ± 21.8 | ** |

* = statistically significant P <.05
** = statistically significant p < .005
*** = statistically significant p < .0005
N.S. = not statistically significant

**Table 15: Summary of width changes in SARPE group**

| | Mean Expansion | | P | Mean Relapse | | P |
|---|---|---|---|---|---|---|
| **Posterior Skeletal Change** | Absolute (mm) | 0.50 ± 0.24 | * | Absolute (mm) | 0.80 ± 0.54 | NS |
| | Relative Expansion (%) | 1.71 ± 0.82 | * | Relative Relapse (%) | 2.71 ± 1.90 | NS |
| | | | | Relapse Rate (%) | 146.9 ± 81.8 | * |
| **Anterior Skeletal Change** | Absolute (mm) | 2.25 ± 1.79 | NS | Absolute (mm) | -0.74 ± 0.63 | NS |
| | Relative Expansion (%) | 10.2 ± 7.71 | NS | Relative Relapse (%) | -2.93 ± 2.29 | NS |
| | | | | Relapse Rate (%) | -32.5 ± 32.5 | *** |
| **Intermolar Width** | Absolute (mm) | 10.0 ± 1.40 | *** | Absolute (mm) | -1.86 ± 1.75 | NS |
| | Relative Expansion (%) | 35.7 ± 8.39 | ** | Relative Relapse (%) | -4.81 ± 4.51 | NS |
| | | | | Relapse Rate (%) | -18.4 ± 16.4 | NS |
| **Intercanine Width** | Absolute (mm) | 5.33 ± 2.42 | * | Absolute (mm) | -0.56 ± 0.38 | NS |
| | Relative Expansion (%) | 28.6 ±17.7 | * | Relative Relapse (%) | -2.26 ± 1.64 | NS |
| | | | | Relapse Rate (%) | -12.7 ± 12.7 | NS |

* = statistically significant P <.05
** = statistically significant p < .005
*** = statistically significant p < .0005
N.S. = not statistically significant

### Ratios of dental to skeletal changes between Le Fort and SARPE groups (Tables 16 and 17)

In the posterior maxilla (Table 16), the Le Fort group had a ratio of dental expansion to skeletal expansion of 0.70, indicating more skeletal change than dental change. The SARPE group had a ratio of 25.20, indicating significantly more dental expansion than skeletal expansion in the posterior maxilla. In the anterior maxilla (Table 17), the Le Fort group had a ratio of dental expansion to skeletal expansion of 0.58, indicating approximately twice as much skeletal change than dental change. In the SARPE group, this ratio was 31.80, indicating significantly more dental change.

The ratios of dental relapse to skeletal relapse in the posterior and anterior maxilla are also presented in Tables 16 and 17. In the posterior maxilla, the Le Fort group had a ratio of dental to skeletal relapse of 1.17, whereas the SARPE group had a ratio of -3.63. This ratio in the SARPE group was due to the finding that between T1 and T2, an increase in width was observed. In the anterior maxilla, the Le Fort group had a ratio of dental to skeletal relapse of 2.25, indicating more dental change than skeletal change. Finally, in the SARPE group, the ratio of dental to skeletal relapse in the anterior maxilla was 4.86, also indicating more relapse in the dentition when compared to the maxillary skeleton.

**Table 16: Ratio of dental to skeletal change in the posterior maxilla**

| | Le Fort | SARPE | P |
|---|---|---|---|
| **Dental Expansion/Skeletal Expansion** | 0.70 (SD = ± 0.41) | 25.2 (SD = ± 15.8) | * |
| **Dental Relapse/ Skeletal Relapse** | 1.17 (SD = ± 0.80) | -3.63 (SD = ± 3.70) | * |

**Table 17: Ratio of dental to skeletal change in the anterior maxilla**

| | Le Fort | SARPE | P |
|---|---|---|---|
| **Dental Expansion/Skeletal Expansion** | 0.58 (SD = ± 0.38) | 31.8 (SD = ± 59.4) | * |
| **Dental Relapse/ Skeletal Relapse** | 2.25 (SD = ± 3.41) | 4.86 (SD = ± 8.10) | NS |

## DISCUSSION

In skeletally non-growing individuals, the midpalatal suture has fused, and there is marked resistance from the other maxillary articulations to transverse expansion.[6,16,36,42,43,47,60,62] Surgical intervention has been advocated to overcome the resistive forces to maxillary expansion in these individuals, and has been used successfully in the treatment of MTD.

To date, there have been numerous publications describing a variety of surgical techniques for correction of MTD, ranging from limited maxillary osteotomies to complete Le Fort I osteotomy with pterygomaxillary separation. The expansion and relapse rates of these surgical procedures have also been widely discussed in the literature, however, there appears to be little agreement among various investigators.[10-12,14-16,18,34,64,75]

In the field of orthodontics and craniofacial surgery, the use of CBCT for measurement and quantification is not original.[64] However, a large majority of studies evaluating surgical expansion of the maxilla use conventional cephalograms and plaster dental models.[11,12,16-18] In addition, previous studies used landmarks at the level of the dentoalveolus and dentition to represent expansive and narrowing changes in the maxillary skeleton. Measurements made at the levels of the dentoalvelous and dentition are subject to great variability as the dentition is in a constant state of change during the course of orthodontic treatment, and may not be a reliable indicator of the changes occurring in the maxilla.

The use of CBCT provides the observer with the option of a three-dimensional reconstruction as well as multiplanar analysis capabilities, allowing for direct visualization and evaluation of internal structures.[64] Podesser *et al*.,[62] showed in their study that computed tomography is a powerful and reliable tool for quantifying transverse changes in the maxilla. The authors demonstrated that nearly all parameters presented high reproducibility and confirmed statistical suitability.[62]

**Anatomical landmarks**

In the present study, the anatomic parameters were selected to represent transverse skeletal changes and transverse intra-arch dental changes in the anterior and posterior regions of the maxillary complex. The palatine canals were evaluated as possible anatomic landmarks for measuring posterior maxillary width changes, and the piriform aperture was evaluated as a possible anatomical feature from which to measure anterior maxillary width changes. Intermolar and intercanine distances were used to measure width changes at the level of the dentition. Although these dental landmarks have been used extensively in previous studies to represent maxillary width changes, their use in a CBCT format were also tested statistically. In the interest of reproducibility of results, the anatomic landmarks chosen must be easily recognizable, and selected measurements must demonstrate high inter- and intra-observer reliability.

The decision to use the palatine foramina for posterior measurement was based on the understanding that it is a stable structure that is unaffected by the surgical procedure.[64] Goldenberg *et al*.,[64,75] and Podesser *et al*.,[62] showed that the greater palatine foramina are reproducible landmarks to use for measuring width changes in the maxilla. The palatine canal is a funnel-shaped structure in a supero-inferior direction, and ends unabruptly in the hard palate. The canal's widest aperture is in its most inferior point, however, the inferior boundary is unclear as it blends in with the hard palate.[76-78] Therefore, from the standpoint of reproducibility, it was vital to define anatomical references in multiple planes of space to clearly convey a specific portion of the highly variable morphology of the canal from which to obtain width measurements. Several combinations of anatomical references and plane views were tested statistically to determine the most reliable grouping to use in the study.

**Reliability**

Statistical confirmation of the reliability of the method was found in the absence of differences between measurements in four subjects, each with three time-points, read on three different occasions by three calibrated observers. The pilot study demonstrated high reproducibility in both the lesser and greater palatine foramina when observed in the axial plane view at the level of the nasal floor, with $R^2$ = 0.92 and 0.87, respectively. In the coronal plane view, the canal was long and funnel-shaped, and it was difficult to reproducibly identify a point along its medial wall to use as a landmark. In the axial plane view, identification of a landmark within the canal was much more manageable as it was often simply a circular form, and its boundaries appeared corticated and clearly defined. Superoinferiorly, it was advantageous to use the nasal floor as a reference as it allowed less variation when selecting a point along the canal. Locating the inferior termination of the canal was difficult because the end of the canal and beginning of the hard palate are not always clearly defined. The greater palatine foramina was used in the second part of the study as opposed to the lesser palatine foramina because it is larger and much easier to locate, and was present in more of the CBCT scans than was the lesser palatine foramina.

The maxillary base width, measured from left to right jugale, demonstrated low reproducibility with an $R^2$ value of 0.62, and was rejected as a reliable measurement of maxillary width. Anteriorly, the incisive canal showed high intra-reader variability and was rejected as a reliable landmark for measuring anterior skeletal width changes. Conversely, the base of the piriform rim was shown to be a reliable landmark to represent anterior skeletal width change, $R^2 = 0.82$. With the exception of the intermolar and intercanine distances, all other measurements were excluded from the second part of the study due to lack of statistical reliability.

**Expansion**

The amount of skeletal expansion observed in this study is not consistent with the amount of skeletal expansion implied in the majority of previous studies. With the exception of the studies conducted by Goldenberg *et al.*,[64,75] all other studies used plaster models or posteroanterior cephalograms for measurement, and thus cannot be used for direct comparison of skeletal changes. In the present study, the posterior maxilla expanded an average of 3.43 ± 1.24 mm in the Le Fort group and 0.50 ± 0.24 mm in the SARPE group. The finding in the SARPE group is similar to that of Goldenberg *et al.*,[75] which reported a mean posterior expansion of 0.34 ± 0.96 mm. Anteriorly, the maxilla expanded an average of 1.94 ± 0.93 mm in the Le Fort group and 2.25 ± 1.79 mm in the SARPE group. This non-uniformity in posterior versus anterior expansion was also observed in the Goldenberg *et al.*,[64] study. Both the present study and the study by Goldenberg *et al*.,[75] did not involve separation of the pterygoid junction during surgery. Separation of the pterygoid [32] plate is associated with high morbidity and carries a significant risk of intraoperative bleeding and damage to adjacent structures, and, therefore, is not performed routinely by craniofacial surgeons.[12,16,37,79] Studies which did include disjunction, i.e., Chamberland *et al*.,[34] showed a more uniform skeletal expansion anteroposteriorly. The pterygomaxillary junction has been shown to be a significant source of resistance to transverse expansion of the maxilla,[40,55,56] and can be related to the disparity between posterior and anterior expansion in this study. Therefore, without separation of the pterygomaxillary junction, the pattern of expansion when using a SARPE procedure is similar to the one described by Wertz[5] in nonsurgical expansion, in which the maxilla expands more anteriorly and inferior as if it were hinged in the posterior and superior aspects.

Dentally, previous studies have shown an increase in intercanine distance ranging from 4.10 – 6.00 mm and an increase in intermolar distance ranging from 5.80 – 8.80 mm as a result of a SARPE procedure.[12-18,80] Our study showed similar values of expansion with an average increase in intercanine distance of 5.33 ± 2.42 mm and an average increase in intermolar distance of 10.0 ± 1.40 mm. These changes in intra-arch width appear to be consistent with previous studies. With respect to segmental Le Fort osteotomy, previous studies have reported intercanine increases ranging from 1.25 – 1.90 mm and intermolar increases ranging from 4.00 – 5.40 mm. [8,11] Our study showed similar values of expansion in the intercanine values averaging 1.01 ± 0.68 mm and lower values in the intermolar category with an average increase of 2.17 ± 0.90 mm. The decrease in posterior dental expansion relative to previous studies may also be related to the absence of separation of the pterygomaxillary junction in our study.

Direct comparison of absolute expansion in the Le Fort group versus the SARPE group is difficult due to the inherent biases related to the indications for selecting one procedure over the other. Based on previous findings related to stability, SARPE procedures are often prescribed in non-growing patients that require transverse expansions of greater than 6 mm, whereas multisegmental Le Fort osteotomy procedures are prescribed in patients that require less than 6 mm of correction.[2,8,11,18] SARPE procedures only allow for transverse corrections: if a patient requires vertical and/or sagittal corrections, a subsequent surgery is performed after orthodontic preparation. In a multisegmental Le Fort osteotomy, corrections in all three planes of space are possible simultaneously. For these reasons, ratios of dental expansion to skeletal expansion were used to contrast the relative changes in the two procedures, as opposed to absolute descriptions.

In the posterior maxilla, the Le Fort group exhibited a ratio of dental to skeletal expansion of 0.70, which indicates that there was more skeletal expansion than dental expansion. The SARPE group was the opposite, with a ratio of dental to skeletal expansion of 25.2, indicating approximately 25 times more dental expansion for every millimeter of skeletal expansion.

In the anterior maxilla, the Le Fort groups had a ratio of dental to skeletal expansion of 0.58, also indicating more skeletal change than dental change. In the SARPE group, the ratio was 31.8, indicating approximately 31 times more dental expansion than skeletal expansion. The findings in the SARPE group are consistent with the results in previous studies which show that the maxilla expands in a hinge-like fashion,[56] with more expansion occurring inferiorly. [30,60]

**Relapse**

There are no other studies that use three-dimensional imaging to report on the skeletal and dental relapse of SARPE and segmental Le Fort osteotomy procedures. The previously mentioned study by Goldenberg *et al*., described effects of expansion, but did not follow up with any data on post-surgical stability. As previously mentioned, with the exception of the studies conducted by Goldenberg *et al*., [64,75] all other studies used plaster models or posteroanterior cephalograms for measurement, and, thus, cannot be used for direct comparison of skeletal changes.

In the Le Fort group, skeletal relapse was generally uniform anteroposteriorly, with a loss of 0.86 ± 0.42 mm (26.0%) anteriorly and 0.55 ± 0.55 mm (24.6%) posteriorly. In the SARPE group, there was an increase in width in the posterior maxilla from T1 to T2. The reason for this finding is unclear. A plausible explanation may be related to the possible relocation of the centers of rotation within the maxilla following the various osteotomies to reduce resistance to expansion. A study by Braun *et al*.,[57] identified the center of rotation of the maxillary complex during orthopedic expansion to be in the area of the frontonasal suture. However, this study was conducted without the influence of surgical cuts which are likely to cause the individual bony segments to have individual centers of rotation. If the centers of rotation are relocated in an outward direction toward the area of the lateral osteotomy, a Hyrax appliance delivering lateral forces on the dentition may create a moment of force which over time may cause the bony segments to separate further, resulting in expansion from T1-T2, rather than relapse. Anterior skeletal relapse in the SARPE group was a mean of 0.74 ± 0.63 mm (32.5%).

Dentally, previous studies have shown relapse rates ranging from 0.20 – 1.10 mm (4 – 20%) of the intercanine distance, and 0.00 – 2.90 mm (0-33%) of the intermolar distance as a result of SARPE procedures. [12-18,80] Our study showed a mean relapse of 0.56 ± 0.38 mm (12.7%) at the canines and 1.86 ± 1.75 mm (18.4%) at the molars. The small sample size in the SARPE group, however, did not provide enough power to arrive at statistical significance for measures of dental relapse in the SARPE group. With respect to segmental Le Fort osteotomy, previous studies have reported relapse rates of 0.10mm (5%) of intercanine distances and a range of 2.00 – 2.60 mm (48-50%) of intermolar distances. [64,75] In our study, there was more relapse at the canines with a mean relapse of 0.39 ± 0.24 mm (43.0%) and less relapse at the molars with a mean relapse of 0.77 ± 0.38 mm (37.9%).

Direct comparison of absolute relapse in the Le Fort group versus the SARPE group is also problematic for the same biases mentioned before related to procedure selection. In contrast, the ratio of dental relapse to skeletal relapse allows us to compare the two surgical procedures. In the posterior maxilla, the Le Fort group had a ratio of 1.17, indicating slightly more dental relapse than skeletal relapse. One possible explanation for this observation may be related to the rigid internal fixation of the bony segments. In the SARPE group, the ratio was -3.63, indicating that more change occurred at the dentition. However, since there was an increase in width from T1 to T2, the calculated ratio is negative.

In the anterior maxilla, the ratio of dental relapse to skeletal relapse in the Le Fort group was 2.25, indicating more dental relapse than skeletal relapse. As stated before, this observation may be related to the anterior rigid fixation occurring at the piriform rim. In the SARPE group, the ratio was 4.86, which indicates more dental relapse than skeletal relapse. Overall, the SARPE group demonstrated more change at the level of the dentition during expansion and relapse, with a significant differential occurring during expansion. The Le Fort group demonstrated more skeletal change during expansion, and more dental change during relapse. The findings in the relapse category are generally consistent with the trends presented in previous literature, with significantly more relapse occurring dentally. [10,34,75] The relapse observed in the Le Fort group are most consistent with the findings of Phillips[11] (48%) and Proffit[8] (50%). In the SARPE group, the relapse observed is most consistent with the findings of Berger[14] (17%) and Anttila[13] (18%).

It is important to note that only relapse at the level of the dentition may be compared to previous studies, as our method has never been used in evaluating skeletal relapse.

**Study Limitations**

A sample size of thirteen is within the range of previous studies that reported on the expansion and relapse related to SARPE and Segmental Le Fort Osteotomy, with samples ranging from twelve to twenty. [8,12,17,18,34,64] Unfortunately, after excluding patients with incomplete data sets and dividing the research subjects into respective subcategories of nine Le Fort and four SARPE , the power of statistical analysis was greatly reduced in revealing significant outcomes where they exist, particularly in the SARPE group.

The ages of the subjects varied greatly, ranging from 17.1 – 43.8 in the Le Fort group and 17.0 – 23.2 in the SARPE group. There was also great variation in the amount of days that passed between the surgical date and the T1 scan, ranging from 5 days to 28 days, and between the T1 scan and the T2 scan, ranging from 187 days to 369 days.

### Directions for future study

Our results indicate that there may be less transverse expansion in the maxillary skeleton than was previously thought, especially when the pterygomaxillary junction is left intact during surgery. Additional investigation of the skeletal effects of expansion when the pterygomaxillary *is* separated is indicated. Furthermore, a study with a larger and more uniform sample may shed some light on the skeletal changes that take place during surgical expansion.

To date, there has been no standard for 3D superimposition using CBCT imaging. Although our study uses 3D imaging to study the internal structures of the maxilla, we reduced volumetric data into planar views and constructed linear measurements, and therefore, we did not take full advantage of the power of 3D imaging. Once an accurate and repeatable method for 3D superimposition on the cranial base is established, future investigation will be able to quantify changes in terms of volumes and surface areas, significantly enhancing our understanding of the movements that occur during expansion.

As previously mentioned, the biomechanics and force systems involved in SARPE and Segmental Le Fort procedures are not well understood. Studies such as those by Shetty,[40] Jafari,[55] and Holberg[56] have investigated the underlying force distribution and trajectories associated with maxillary expansion, but do not address the rotation or translation of bony segments as a result of surgical osteotomy. Future studies that combine all the aforementioned voids in our current knowledge will help our understanding of the biomechanics involved in maxillary expansion and will allow us to predict and ultimately control our surgical outcomes.

## CONCLUSIONS

- Surgical expansion of the maxilla in the transverse dimension without performing separation of the pterygomaxillary junction resulted in less than 1 mm of skeletal expansion.
- During expansion with a multisegmental Le Fort procedure, more expansion occurred skeletally than dentally, with a posterior and anterior ratio of dental:skeletal expansion of 0.70 and 0.58, respectively.
- During expansion with a SARPE procedure, significantly more expansion occurred dentally than skeletally, with a posterior and anterior ratio of dental:skeletal expansion of 25.2 and 31.8, respectively.
- In both groups, relapse was more dental than skeletal, with the SARPE group showing a higher ratio of dental:skeletal change.
- The forces generated by expansion via a Hyrax appliance in a SARPE procedure may cause a slight increase in width from T1 to T2 due to changes in the biomechanical system resulting from osteotomy.

## REFERENCES


1. Bishara SE. Textbook of Orthodontics. Philadelphia, Pa.: Saunders; 2001.

2. Proffit WR, Phillips C, Dann Ct. Who seeks surgical-orthodontic treatment? Int J Adult Orthodon Orthognath Surg 1990;5:153-160.

3. McNamara JA. Maxillary transverse deficiency. Am J Orthod Dentofacial Orthop 2000;117:567-570.

4. Cleall JF, Bayne DI, Posen JM, Subtelny JD. Expansion of the Midpalatal Suture in the Monkey. Angle Orthod 1965;35:23-35.

5. Wertz RA. Skeletal and dental changes accompanying rapid midpalatal suture opening. Am J Orthod 1970;58:41-66.

6. Melsen B. Palatal growth studied on human autopsy material. A histologic microradiographic study. Am J Orthod 1975;68:42-54.

7. Lines PA. Adult rapid maxillary expansion with corticotomy. Am J Orthod 1975;67:44-56.

8. Proffit WR, Turvey TA, Phillips C. Orthognathic surgery: a hierarchy of stability. Int J Adult Orthodon Orthognath Surg 1996;11:191-204.

9. Betts NJ, Sturtz DH, Aldrich DA. Treatment of transverse (width) discrepancies in patients who require isolated mandibular surgery: the case for maxillary expansion. J Oral Maxillofac Surg 2004;62:361-364.

10. Marchetti C, Pironi M, Bianchi A, Musci A. Surgically assisted rapid palatal expansion vs. segmental Le Fort I osteotomy: transverse stability over a 2-year period. J Craniomaxillofac Surg 2009;37:74-78.

11. Phillips C, Medland WH, Fields HW, Jr., Proffit WR, White RP, Jr. Stability of surgical maxillary expansion. Int J Adult Orthodon Orthognath Surg 1992;7:139-146.

12. Byloff FK, Mossaz CF. Skeletal and dental changes following surgically assisted rapid palatal expansion. Eur J Orthod 2004;26:403-409.

13. Anttila A, Finne K, Keski-Nisula K, Somppi M, Panula K, Peltomaki T. Feasibility and long-term stability of surgically assisted rapid maxillary expansion with lateral osteotomy. Eur J Orthod 2004;26:391-395.

14. Berger JL, Pangrazio-Kulbersh V, Borgula T, Kaczynski R. Stability of orthopedic and surgically assisted rapid palatal expansion over time. Am J Orthod Dentofacial Orthop 1998;114:638-645.

15. Northway WM, Meade JB, Jr. Surgically assisted rapid maxillary expansion: a comparison of technique, response, and stability. Angle Orthod 1997;67:309-320.

16. Stromberg C, Holm J. Surgically assisted, rapid maxillary expansion in adults. A retrospective long-term follow-up study. J Craniomaxillofac Surg 1995;23:222-227.

17. Bays RA, Greco JM. Surgically assisted rapid palatal expansion: an outpatient technique with long-term stability. J Oral Maxillofac Surg 1992;50:110-113; discussion 114-115.

18. Pogrel MA, Kaban LB, Vargervik K, Baumrind S. Surgically assisted rapid maxillary expansion in adults. Int J Adult Orthodon Orthognath Surg 1992;7:37-41.

19. Ricketts RM. The wisdom of the bioprogressive philosophy. Semin Orthod 1998;4:201-209.

20. Vanarsdall RL, Jr. Transverse dimension and long-term stability. Semin Orthod 1999;5:171-180.

21. Proffit WR, Fields HW, Sarver DM. Contemporary Orthodontics. St. Louis, Mo.: Mosby Elsevier; 2007.

22. Cistulli PA, Sullivan CE. Sleep-disordered breathing in Marfan's syndrome. Am Rev Respir Dis 1993;147:645-648.

23. Gorlin RJ, Cohen MM, Hennekam RCM. Syndromes of the Head and Neck. Oxford [England] ; New York: Oxford University Press; 2001.

24. Ye B, Ruan C, Hu J, Yang Y, Ghosh A, Jana S *et al*. A comparative study on dental-arch morphology in adult unoperated and operated cleft palate patients. J Craniofac Surg;21:811-815.

25. Suri L, Taneja P. Surgically assisted rapid palatal expansion: a literature review. Am J Orthod Dentofacial Orthop 2008;133:290-302.

26. Woodside DG, Linder-Aronson S, Lundstrom A, McWilliam J. Mandibular and maxillary growth after changed mode of breathing. Am J Orthod Dentofacial Orthop 1991;100:1-18.

27. Harvold EP, Chierici G, Vargervik K. Experiments on the development of dental malocclusions. Am J Orthod 1972;61:38-44.

28. Haas A. Just the beginning of dentofacial orthopedics. Angle Orthod 1970;57:219-255.

29. Proffit W. Contemporary Orthodontics. St Louis: Mosby, Inc.; 2000.

30. Bishara SE, Staley RN. Maxillary expansion: clinical implications. Am J Orthod Dentofacial Orthop 1987;91:3-14.

31. Bailey LJ, Proffit WR, White R, Jr. Assessment of patients for orthognathic surgery. Semin Orthod 1999;5:209-222.

32. Silverstein K, Quinn PD. Surgically-assisted rapid palatal expansion for management of transverse maxillary deficiency. J Oral Maxillofac Surg 1997;55:725-727.

33. Bailey LJ, White RP, Jr., Proffit WR, Turvey TA. Segmental LeFort I osteotomy for management of transverse maxillary deficiency. J Oral Maxillofac Surg 1997;55:728-731.

34. Chamberland S, Proffit WR. Closer look at the stability of surgically assisted rapid palatal expansion. J Oral Maxillofac Surg 2008;66:1895-1900.

35. Proffit WR, Turvey TA, Phillips C. The hierarchy of stability and predictability in orthognathic surgery with rigid fixation: an update and extension. Head Face Med 2007;3:21.

36. Betts NJ, Vanarsdall RL, Barber HD, Higgins-Barber K, Fonseca RJ. Diagnosis and treatment of transverse maxillary deficiency. Int J Adult Orthodon Orthognath Surg 1995;10:75-96.

37. Woods M, Wiesenfeld D, Probert T. Surgically-assisted maxillary expansion. Aust Dent J 1997;42:38-42.

38. Koudstaal MJ, Poort LJ, van der Wal KG, Wolvius EB, Prahl-Andersen B, Schulten AJ. Surgically assisted rapid maxillary expansion (SARME): a review of the literature. Int J Oral Maxillofac Surg 2005;34:709-714.

39. Fonseca RJ. Oral and Maxillofacial Surgery. Saunders Publishing, Philadelphia, PA, 2000.

40. Shetty V, Caridad JM, Caputo AA, Chaconas SJ. Biomechanical rationale for surgical-orthodontic expansion of the adult maxilla. J Oral Maxillofac Surg 1994;52:742-749; discussion 750-741.

41. Persson M, Thilander B. Palatal suture closure in man from 15 to 35 years of age. Am J Orthod 1977;72:42-52.

42. Timms DJ, Vero D. The relationship of rapid maxillary expansion to surgery with special reference to midpalatal synostosis. Br J Oral Surg 1981;19:180-196.

43. Bell WH, Epker BN. Surgical-orthodontic expansion of the maxilla. Am J Orthod 1976;70:517-528.

44. Jacobs JD, Bell WH, Williams CE, Kennedy JW, 3rd. Control of the transverse dimension with surgery and orthodontics. Am J Orthod 1980;77:284-306.

45. Brown. Surgery of oral and facial diseases and malformations: their diagnosis and treatment including plastic reconstruction, Philadelphia: Lea & Febiger, 1938.

46. Kole H. Surgical operations on the alveolar ridge to correct occlusal abnormalities. Oral Surg Oral Med Oral Pathol 1959;12:515-529 concl.

47. Timms DJ. An occlusal analysis of lateral maxillary expansion with midpalatal suture opening. Dent Pract Dent Rec 1968;18:435-441.

48. Isaacson RJ, Wood JL, Ingram AH. Forces produced by rapid maxillary expansion. Angle Orthod 1964;34.

49. Converse JM, Horowitz SL. The surgical-orthodontic approach to the treatment of dentofacial deformities. Am J Orthod 1969;55:217-243.
50. Steinhauser EW. Midline splitting of the maxilla for correction of malocclusion. J Oral Surg 1972;30:413-422.
51. Kennedy JW, 3rd, Bell WH, Kimbrough OL, James WB. Osteotomy as an adjunct to rapid maxillary expansion. Am J Orthod 1976;70:123-137.
52. Lehman JA, Jr., Haas AJ, Haas DG. Surgical orthodontic correction of transverse maxillary deficiency: a simplified approach. Plast Reconstr Surg 1984;73:62-68.
53. Glassman AS, Nahigian SJ, Medway JM, Aronowitz HI. Conservative surgical orthodontic adult rapid palatal expansion: sixteen cases. Am J Orthod 1984;86:207-213.
54. Chaconas SJ, Caputo AA. Observation of orthopedic force distribution produced by maxillary orthodontic appliances. Am J Orthod 1982;82:492-501.
55. Jafari A, Shetty KS, Kumar M. Study of stress distribution and displacement of various craniofacial structures following application of transverse orthopedic forces--a three-dimensional FEM study. Angle Orthod 2003;73:12-20.
56. Holberg C, Steinhauser S, Rudzki I. Surgically assisted rapid maxillary expansion: midfacial and cranial stress distribution. Am J Orthod Dentofacial Orthop 2007;132:776-782.
57. Braun S, Bottrel JA, Lee KG, Lunazzi JJ, Legan HL. The biomechanics of rapid maxillary sutural expansion. Am J Orthod Dentofacial Orthop 2000;118:257-261.

58. Lee KG, Ryu YK, Park YC, Rudolph DJ. A study of holographic interferometry on the initial reaction of maxillofacial complex during protraction. Am J Orthod Dentofacial Orthop 1997;111:623-632.

59. Redmond WR. Digital models: a new diagnostic tool. J Clin Orthod 2001;35:386-387.

60. Haas AJ. The Treatment of Maxillary Deficiency by Opening the Midpalatal Suture. Angle Orthod 1965;35:200-217.

61. Baccetti T, Franchi L, Cameron CG, McNamara JA, Jr. Treatment timing for rapid maxillary expansion. Angle Orthod 2001;71:343-350.

62. Podesser B, Williams S, Bantleon HP, Imhof H. Quantitation of transverse maxillary dimensions using computed tomography: a methodological and reproducibility study. Eur J Orthod 2004;26:209-215.

63. Loddi PP, Pereira MD, Wolosker AB, Hino CT, Kreniski TM, Ferreira LM. Transverse effects after surgically assisted rapid maxillary expansion in the midpalatal suture using computed tomography. J Craniofac Surg 2008;19:433-438.

64. Goldenberg DC, Alonso N, Goldenberg FC, Gebrin ES, Amaral TS, Scanavini MA *et al*. Using computed tomography to evaluate maxillary changes after surgically assisted rapid palatal expansion. J Craniofac Surg 2007;18:302-311.

65. Waitzman AA, Posnick JC, Armstrong DC, Pron GE. Craniofacial skeletal measurements based on computed tomography: Part I. Accuracy and reproducibility. Cleft Palate Craniofac J 1992;29:112-117.

66. Loubele M, Bogaerts R, Van Dijck E, Pauwels R, Vanheusden S, Suetens P *et al*. Comparison between effective radiation dose of CBCT and MSCT scanners for dentomaxillofacial applications. Eur J Radiol 2009;71:461-468.

67. Mah JK, Danforth RA, Bumann A, Hatcher D. Radiation absorbed in maxillofacial imaging with a new dental computed tomography device. Oral Surg Oral Med Oral Pathol Oral Radiol Endod 2003;96:508-513.

68. Ludlow JB D-LL, Brooks SL. Dosimetry of two extraoral direct digital imaging devices: NewTom cone beam Ct and Orthophos Plus DS panoramic unit. Dentomaxillofac Radiol 2003;32:229-234.

69. Mah J, Hatcher D. Current status and future needs in craniofacial imaging. Orthod Craniofac Res 2003;6 Suppl 1:10-16; discussion 179-182.

70. Danforth RA, Dus I, Mah J. 3-D volume imaging for dentistry: a new dimension. J Calif Dent Assoc 2003;31:817-823.

71. Vannier MW. Craniofacial computed tomography scanning: technology, applications and future trends. Orthod Craniofac Res 2003;6 Suppl 1:23-30; discussion 179-182.

72. Cavalcanti MG, Haller JW, Vannier MW. Three-dimensional computed tomography landmark measurement in craniofacial surgical planning: experimental validation *in vitro*. J Oral Maxillofac Surg 1999;57:690-694.

73. Stratemann S. 3D Craniofacial Imaging: Airway and Craniofacial Morphology Orthodontics. San Francisco: University of California, San Francisco; 2005.

74. Kragskov J, Bosch C, Gyldensted C, Sindet-Pedersen S. Comparison of the reliability of craniofacial anatomic landmarks based on cephalometric

radiographs and three-dimensional CT scans. Cleft Palate Craniofac J 1997;34:111-116.

75. Goldenberg DC, Goldenberg FC, Alonso N, Gebrin ES, Amaral TS, Scanavini MA *et al*. Hyrax appliance opening and pattern of skeletal maxillary expansion after surgically assisted rapid palatal expansion: a computed tomography evaluation. Oral Surg Oral Med Oral Pathol Oral Radiol Endod 2008;106:812-819.

76. Wentges RT. Surgical anatomy of the pterygopalatine fossa. J Laryngol Otol 1975;89:35-45.

77. Methathrathip D, Apinhasmit W, Chompoopong S, Lertsirithong A, Ariyawatkul T, Sangvichien S. Anatomy of greater palatine foramen and canal and pterygopalatine fossa in Thais: considerations for maxillary nerve block. Surg Radiol Anat 2005;27:511-516.

78. Howard-Swirzinski K, Edwards PC, Saini TS, Norton NS. Length and geometric patterns of the greater palatine canal observed in cone beam computed tomography. Int J Dent;2010.

79. Cureton SL, Cuenin M. Surgically assisted rapid palatal expansion: orthodontic preparation for clinical success. Am J Orthod Dentofacial Orthop 1999;116:46-59.

80. Schimming R, Feller KU, Herzmann K, Eckelt U. Surgical and orthodontic rapid palatal expansion in adults using Glassman's technique: retrospective study. Br J Oral Maxillofac Surg 2000;38:66-69.

**Publishing Agreement**

*It is the policy of the University to encourage the distribution of all theses, dissertations, and manuscripts. Copies of all UCSF theses, dissertations, and manuscripts will be routed to the library via the Graduate Division. The library will make all theses, dissertations, and manuscripts accessible to the public and will preserve these to the best of their abilities, in perpetuity.*

***Please sign the following statement:***

*I hereby grant permission to the Graduate Division of the University of California, San Francisco to release copies of my thesis, dissertation, or manuscript to the Campus Library to provide access and preservation, in whole or in part, in perpetuity.*

Author Signature

6/8/11

Date